



Norwegian University of
Science and Technology

Development of Kraft Lignin and Coating Technique to Prepare Coated Urea Fertilizers with Increased Nutrient Use Efficiency

Xueyan Xu

Chemical Engineering

Submission date: July 2017

Supervisor: Kristin Syverud, IKP

Co-supervisor: Jiebing Li, RISE

Norwegian University of Science and Technology
Department of Chemical Engineering

Preface

This article is a Master's thesis in the department of Chemical Engineering at NTNU as part of the joint study program Nordic 5 polymer technology together with KTH during the spring semester of 2017. It is made under cooperation with the Research Institutes of Sweden (RISE). The idea was brought up by Jiebing Li, the co-supervisor and responsible person in RISE. He has been working with lignin and relevant topics and projects for many years. This study is based on what he and his co-workers have been working with before. All the experiments and measurements were conducted by me in the lab at Research Institutes of Sweden/Bioeconomy in 2017.

Stockholm, 2017-06-30

Xueyan Xu

Acknowledgment

The study of this Master's thesis work has been proceeded since the 29th of January till the 30th of June. It has been an interesting journey with many hours of computer work and laboratory work. It has been an unforgettable period with gaining new experiences and knowledge all the time.

I would like to thank the following persons for their great help during my thesis work. My supervisor Kristin Syverud in NTNU has been giving me a lot of support during this study. Thank you for your guidance during different meetings. I would like to thank my co-supervisor Dr. Jiebing Li. Thank you for all the help in every aspects of my academic work. Your patience guidance gave me an overview of how a researcher should work for his/her project. Thank you for the detailed and clear explanation on different aspects of project research. Secondly, I want to thank Jasna Stevanic-Srndovic at the Research Institutes of Sweden/Bioeconomy for giving me a lot of help and sharing the knowledge in FTIR data analysis. I also want to express my gratitude to Professor Karin Odelius at the Department of Fibre and Polymer Technology in KTH, thanks for the patient reminding and controlling of the schedule of the work. Thank you also for giving me many suggestions in choosing coating materials. Ph.D Yading Zhao at the Department of Fibre and Polymer Technology in KTH has also helped me a lot with equipment training and data analyzing. All the Master's students who worked along with me on their projects in RISE/Bioeconomy are acknowledged for their warm company and giving me many help when I was not in a good shape. At last, I would like to thank Luca Bessegato, for all the love he has showed to me, and all the gentle care and protection he has been giving me. This work will not be finished without you.

Finally, I declare that this is an independent work, according to the exam regulations of the Norwegian University of Science and Technology (NTNU).

Xueyan Xu

Abstract

Coating urea to prepare controlled release N-fertilizer has been considered as an effective way to increase its nutrient use efficiency, thus reduce its waste and the consequent harmful environmental impacts. Inorganic sulphur and synthetic polymers have been used in the industry as coating materials together with utilization of various types of expensive coating equipment which commonly requires also complicated technical setup and controls. As development trends, biopolymers are attention-grabbing to replace the synthetic polymers. Alternative simple coating technique is also desired. So far, polylactic acid (PLA) has been reported as a more promising biopolymer than several synthetic polymers for coating. On the other hand, highly purified industrial softwood kraft lignin (SKL) produced after LignoBoost process is now available in a large quantity, which should also be a promising biopolymer for the coating application. Aiming at increase of the efficiency of PLA-coated urea and development of alternative coating technique to generally make the preparation of control-released fertilizer more effective, economic and environmentally sustainable, in this study, SKL has been used in a PLA-SKL blending form as complex coating material and simple dip-coating technique has been investigated and applied.

In order to lower the wettability of PLA-SKL coat layer, four different anhydrides, namely acetic anhydride, palmitic anhydride, lauric anhydride and trifluoroacetic anhydride, were used to esterify SKL to form AcSKL, PaSKL, LauSKL and TFASKL respectively before its utilization. NMR and FTIR analyses showed that the esterification reactions have been completed for AcSKL and PaSKL. LauSKL was partly esterified due to the low charge of lauric anhydride reagent, while TFASKL was not esterified expectantly due to the steric hindrance between the three F atoms and polymeric SKL.

In order to obtain organically bound nitrogen structure to also create slow-release type of N-fertilizer, Mannich reaction on SKL using diethylamine was also conducted to prepare ManSKL. The reaction was completed as shown by NMR and FTIR spectroscopy. To bring further functionality of metal chelation to open the possibility to also bring essential trace element into the

final fertilizer, ethylenediaminetriacetic acid (ED3A) was synthesized and further used via Mannich reaction to modify SKL to form ED3ASKL. ED3A is not commercially available and it was synthesized successfully with an environmentally friendly method from commercial EDTA and the structure was verified by NMR spectroscopy. However, the Mannich reaction using ED3A was not very successful as shown by product's NMR and FTIR spectra. In a comparison experiment using vanillyl alcohol as a lignin model structure, ED3A was successfully coupled onto the vanillyl alcohol structure as shown by NMR and FTIR spectra. Apparently there was a severe steric hindrance from SKL for the Mannich reaction using the larger molecule of ED3A than diethylamine for Mannich reaction.

For utilization of dip-coating technique, dichloromethane (DCM) and tetrahydrofuran (THF) were chosen to dissolve PLA and SKL or the modified SKL respectively. Cast films of PLA/modified lignin complex were prepared using Teflon Petri-dishes. The optimal concentration of PLA in DCM and the effect of DCM/THF ratios on the prepared cast film which expectantly represents the quality of the complex coat in the coated urea were compared with SEM images and contact angle determination. It has been found that a 30 wt% of PLA in DCM was the best and this solution mixed with modified lignin solution (6 % in THF) in a ratio of DCM/THF =3/2 (v/v) had the best film performances and water barrier properties. Generally, the cast films from PLA/modified lignin complexes showed better properties compared with the neat PLA cast film. No pores and cracks were found on the surface. Comparatively, the LauSKL film showed the most homogeneous surface. But the AcSKL film had the best water barrier properties.

The PLA/modified lignin complex coated urea was then prepared by dip-coating process. The coat thickness and weight increase showed statistically positive correlations against the repeating times of the dip-coating process. The coating layer also showed one single layer structure. The speed of urea releasing for coated urea was tested and the results showed that it was much slower than the un-coated or PLA-coated urea. The single-layered PLA/AcSKL and PLA/ManSKL were both observed with sound properties in delaying the release of urea cores in water.

Conclusively, the PLA/modified SKL coated urea fertilizers prepared by dip-coating technique demonstrated in this study have highly efficiency with better effects of water barrier, organically N slow release, and nitrification inhibiting (due to free phenolic functional groups)

properties. Both SKL and the dip-coating technique are promising in the fertilizer applications.

List of abbreviations and symbols

δ_d Dispersion solubility parameter

δ_h Hydrogen bonding solubility parameter

δ_p Polar solubility parameter

δ_t Total Hansen solubility parameter

ν_{ref} Absolute resonance frequency of standard reference

ν_{sample} Absolute resonance frequency of the sample atom

AAPFCO Association of American Plant Food Control Officials

AcSKL Acetylated SKL

ASA Alkenyl succinic anhydride

CDU Crotonaldehyde-urea

DCM Dichloromethane

EC Ethylcellulose

ED3A Ethylenediaminetriacetic acid

ED3ASKL ED3A modified SKL

ED3AVA ED3A modified vanillyl alcohol

EDTA Ethylenediaminetetraacetic acid

FTIR Fourier transform infrared spectroscopy

G Guaiacyl

H *p*-hydroxyphenyl alcohol/unit

HSP Hansen solubility parameter

HSQC Heteronuclear single-quantum correlation spectroscopy

IBDU Urea-isobutyraldehyde

K Permeability coefficient

LauSKL Laurylated SKL

ManSKL Mannich reaction product from SKL using diethylamine

MAS Magic angle spinning

MMD Molecular mass distribution

NMR Nuclear magnetic resonance

NUE Nutrient use efficiency

OPD Optical path difference

PaSKL Palmitylated SKL

PBS Polybutylene succinate

PDI Polydispersity index

PLA Poly lactic acetate

PSU Polymer coated slow released urea

PVA Polyvinyl alcohol

S Syringyl

SCU Sulphur-coated urea

SEM Scanning electron microscopy

SKL Softwood kraft lignin

TFAA Trifluoroacetic anhydride

TFASKL Trifluoroacetylated SKL

THF Tetrahydrofuran

UF Urea-formaldehyde

Contents

Preface	i
Acknowledgment	ii
1 Background and theory	2
1.1 Slow and controlled-release fertilizers	2
1.1.1 Classification	2
1.1.2 Coating methods	4
1.1.3 Coating materials	7
1.2 Lignin	9
1.2.1 Native lignin	9
1.2.2 LignoBoost process	11
1.2.3 The Mannich reaction	13
1.3 Lignin-modified slow-released fertilizers	14
1.4 Characterization methods	16
1.4.1 NMR spectroscopy	16
1.4.2 Contact angle test	19
1.4.3 SEM spectroscopy	20
1.4.4 FTIR spectroscopy	21
1.5 Objectives	22
2 Experimental	24
2.1 Chemicals and materials	24
2.2 Esterification of lignin	25
2.3 The Mannich reaction	26

<i>CONTENTS</i>	1
2.3.1 Reaction between diethylamine and lignin	26
2.3.2 Reaction between ED3A and lignin	26
2.4 NMR spectroscopy	28
2.5 FTIR analysis	29
2.6 Film casting	30
2.7 Contact angle tests	30
2.8 Scanning electron microscopy (SEM) tests	31
2.9 Urea coating and water immerse tests	31
3 Results and discussion	32
3.1 Lignin modifications	32
3.1.1 Original SKL lignin	32
3.1.2 Esterifications of lignin	37
3.1.3 Amination of lignin: the Mannich reactions	46
3.2 Coating urea pellets	55
3.2.1 Solvent selection	56
3.2.2 Film casting and its evaluations	57
3.2.3 Dip-coating results	66
3.2.4 Urea release	67
4 Summary	71
4.1 Summary and Conclusions	71
4.2 Recommendations for Further Work	72
Bibliography	74
A Calculation of OH from ³¹P NMR spectra	79
B NMR spectra of ED3A	81

Chapter 1

Background and theory

1.1 Slow and controlled-release fertilizers

1.1.1 Classification

Nitrogen (N) is a chemical element presenting in all organisms. It works as an energy transform molecule in the body system. Crops, as a necessary supply to all the human beings, also need nitrogen to maintain growth. Looking from the mechanism of plants nutrition utilization, plants take nutrition from the surrounding soil, but the soil and plants are two antagonistic systems competing for the available nutrients in the soil or the nutrients applied by field owners. This competition is the main issue and a primary reason why only a portion of the nutrients are taken by the crops. For example, for many years, N fertilizers have widely been used to provide nutrients to plants in order to sustain optimal crop yield. However, with the increasing needs of crops around the world and the low efficiency of N fertilizers, finding a good way to improve the use efficiency of N fertilizer, while keeping the cost low, becomes more and more important for many chemists, fertilizer producers, and users. Among different N fertilizers, urea ($\text{CO}(\text{NH}_2)_2$) has become one of the mostly used nitrogenous fertilizers with its favourable commercially availability and high N content value.

The nutrient use efficiency (NUE) is normally calculated as the ratio of the amount of nutrients used up by plants and crops from the surrounding soils over the nutrients applied on the soil within the same period. For nitrogenous fertilizers such as urea, this ratio can only be

around 50 % to 70 % during the first year according to the report from [Finck \(1992\)](#). In fact, the losses through immobilization, denitrification/volatilization, and leaching are more significant with nitrogen ([Trenkel \(1997\)](#)).

Urea and other most commonly used N fertilizers can easily be harmful to the environment if they are misused. The main environmental impacts have been linked to the pollution of waters due to the high concentration of soluble N forms in the N fertilizers and the pollution of the atmosphere with nitrous oxide, other oxides of nitrogen, and ammonia ([Byrnes \(1990\)](#)). These undesired conversions and losses of fertilizers may cause substantial economic losses and environmental damages. Therefore, developing modified urea fertilizers in order to reduce the losses of N nutrients has been a challenge to fertilizer industry.

One technique that has been investigated is the addition of nitrification inhibitors. During nitrification, the ammonium in the soil is converted into nitrite (NO_2^-) which is further transformed into nitrate (NO_3^-) by bacterial oxidation ([Trenkel \(1997\)](#)). The addition of nitrification inhibitors can help with lowering the speed of bacterial activity. Therefore, it can help with controlling the leaching of nitrate and reducing emissions of N_2O and NO_x ([Bronson et al. \(1992\)](#)). Another possible solution is using slow or controlled-release and stabilized fertilizers. The definition of slow and controlled-released fertilizer is as follow (according to the AAPFCO, [Association of American Plant Food Control Officials \(1997\)](#)):

"a fertilizer containing a plant nutrient in a form which delays its availability for plant uptake and use after application, or which extends its availability to the plant significantly longer than a reference 'rapidly available nutrient fertilizer' such as ammonium nitrate or urea, ammonium phosphate or potassium chloride. Such delay of initial availability or extended time of continued availability may occur by a variety of mechanisms. These include controlled water solubility of the material by semi-permeable coatings, occlusion, protein materials, or other chemical forms, by slow hydrolysis of water-soluble low molecular weight compounds, or by other unknown means."

Diverse groups of slow and controlled-released fertilizers have been made to meet these requirements. Among these, condensation products of urea and urea-aldehydes and the coated fertilizers are the two main groups with comprehensive manufacture processes.

The conventional condensation products of urea and aldehydes consists of urea-formaldehyde (UF, 38 % N), urea-crotonaldehyde (CDU, 32.5 % N) and urea-isobutyraldehyde (IBDU, 32 % N) (Goertz (1993)). Though UF has the largest market now due to its relatively lower cost in manufacture compared with the other two types, all of these fertilizers showed higher properties compared with the bare urea pellet. Some methods have also been investigated to further increase the efficiency of conventional UF. Yamamoto et al. (2016) have developed a nano-composite material based on exfoliation of montmorillonite and made it into a matrix of urea/urea-formaldehyde polymer. Meanwhile, Pereira et al. (2015) has developed a fertilizer made by urea nanocomposites associated with an exfoliated clay mineral, prepared from various concentrations of hydrophilic or hydrophobic polymers. These new fertilizers have showed better mechanical resistance, higher nutrient efficiency and bigger supplement of large novel nitrogen fertilizers with lower nitrous oxide emissions in the field.

Coated/encapsulated controlled-release fertilizers have also been put on production in many plants. A protective layer is made surrounding the conventional soluble fertilizer such as urea in order to control the rate of dissolution and the nutrients release. Normally the outer layer of these fertilizers is made to be water insoluble by coating. Sulphur, polymeric materials and combination of polymeric materials and sulphur are the three main groups of coating layers. Sulphur-coated urea (SCU) was at first brought forward in the 1960s to 1980s because of its fine slow-release properties. But later it was found that the high coating weight ratio of sulphur results in a lower N content (35 %-37 %) than uncoated urea (46 %) (Young (1974)). The relatively higher SCU expense on the SCU transport leads to an increasing demand of fertilizers with lower ratio of coating layer and higher N contents, especially in developing countries. Later, urea with double-layered polymer-sealed S coating was investigated and produced by some companies such as "TriKote" by Pursell and "Poly-S" by Scotts (Chien et al. (2009)). This urea pellet has a relatively light coating layer and similar effects as the one coated with sulphur. Thus, the problem of extra expenses in urea transportation could be solved.

1.1.2 Coating methods

Selection of coating methods is usually based on the components used and economic constraints (Shipway (2006)). The properties of the coating materials (thickness and surface rough-

ness) and the true material properties such as hardness and toughness all primarily contribute to the final functions of coating.

Rotary drum, pan coater and fluidized bed spraying techniques are the three techniques usually used in the coating for slow-released fertilizers (Devassine et al. (2002)). However, these techniques have their inherent weaknesses. For the rotating drum process, for example, a large amount of coating materials need to be added to reach an uniform thickness of the coating layer. This causes high prices of the final fertilizers.

In the rotating pan process, on the other hand, many factors such as motion of granules bed, air ducts of hot air and cold air, spray gun and motion of pan need to be controlled. All these factors will influence the final coating layer properties. In fact, most of the coated urea fertilizers have rough surface with large amount of pores and defects after this process.

Typically, the fluidized bed spray process can ensure the uniform coating layer thickness, but it has even higher requirements of granule sizes, coating materials and processing parameters compared to the other techniques. For example, Hede et al. (2009) have investigated the influence of the drying speed and spray rate on the agglomeration effect of PVA (polyvinyl alcohol)/SiO₂ coated granules. The results showed that the agglomeration tendency increased as the drying speed decreases. Therefore, it is hard to balance different factors in reality to obtain well-separated coated fertilizers by using the fluidized bed. Figure 1.1 shows the summarized factors to be considered for fluidized bed spray coating process.

Overall, new techniques with low cost and high efficiency still need to be investigated, especially for using uneven sizes granules such as urea fertilizers..

One simple coating method, dip-coating method has given rise to our interest. The method is commonly used for candle preparation. By repeat-dipping the inner fabric into the bath of coating, it forms a bulk with several layer of thin films outside. This process is repeated until the candle reaches its desired final thickness. For a 3D structure such as urea pellets, it can simply conducted by immersing and removing from the solution of coating material. After the excess solution drained from the surface, the coating layer of fertilizers is formed after evaporation of the coating solvent. Compared with the fluidized bed and rotating pan, dip-coating method is easier to conduct and has relatively lower requirements in the equipment settings. Therefore, dip-coating process could be, in this case, considered as one potential convenient method to

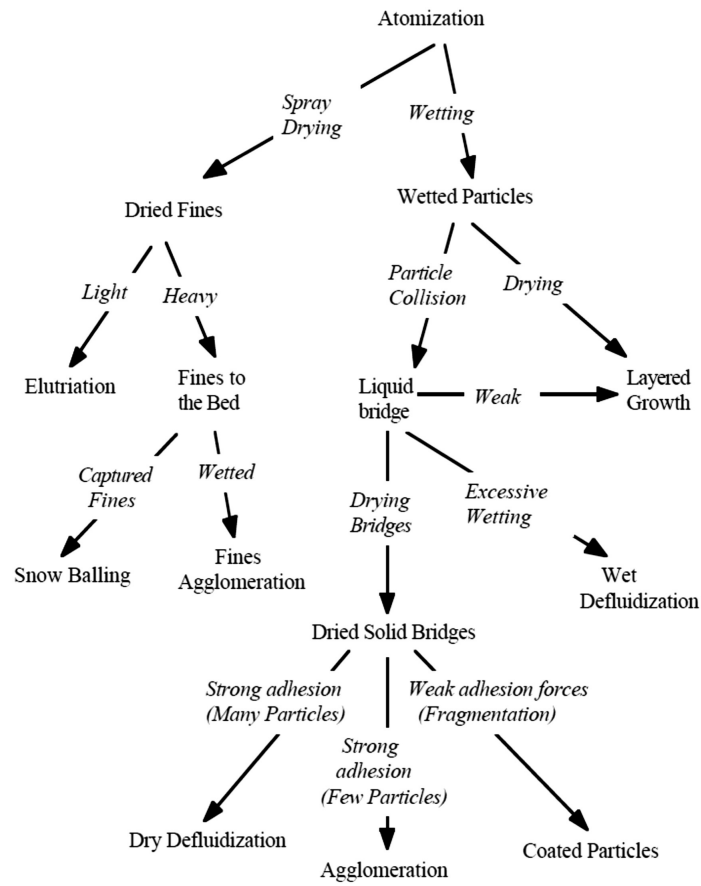


Figure 1.1: Flow chat of fluidized bed coating process cited from [Naz and Sulaiman \(2016\)](#).

proceed coating outside urea pellets. Compared to other coating methods, the effect of the dip-coating technique is more closely related to the coating material used. Therefore it is more important to select correct coating material and have the properties of selected coating material evaluated to reach the best coating results. The coating effects can be tested by evaluating cast films as well as contact angle tests, since the coating layer of dip-coating is usually formed in a similar manner to the film formation from the solution.

1.1.3 Coating materials

Nowadays, with the development of new macro-molecular materials, more and more polymers have been used as fertilizer coating materials. It has been proved that the polymer coated slow released urea (PSU) has better qualities and efficiency compared with SCU when it is used in crops (Noellsch et al. (2009)). In addition, the effects of the coating layers and the releasing rates depend on the polymers used. However, synthetic polymers are known as materials that are hard to be degraded. This places the usage of polymer in a dilemma. If fertilizer users want to guarantee the longevity of polymer coated urea and longer supply of nutrients, the coating polymer should have good bio- and chemical resistances. Meanwhile, the polymer coated layer left in the soil may cause problems in the long run.

For this reason, biodegradable and bio-polymers were considered as a new approach as coating materials to make slow-released fertilizers. Devassine et al. (2002) classified some common biodegradable polymers as a function of their properties like water vapour and liquid barrier. Permeability coefficient (K), which is the representation of hydrophilicity, has been calculated out to compare different coating polymers. The conclusion is that polylactic acid (PLA) and biopols are the two polymers which showed the best performance in water barrier for out-layer coating ($K=1700 \times 10^{-13}$, and $K=157-180 \times 10^{-13} \text{ cm}^2 \cdot \text{s}^{-1} \cdot \text{Pa}^{-1}$, respectively), as shown in Figure 1.2. The results also showed that polymer crystallinity is critical for reduction of water vapour permeability. In addition, biopolymers, such as lignin, cellulose and starch (Min et al. (2005)) have also been studied because of their low price and biodegradable properties. However, most of these biopolymers cannot be used directly as coating materials due to their natural structural defects. Instead, some physical or chemical modifications need to be proceeded before they can be used.

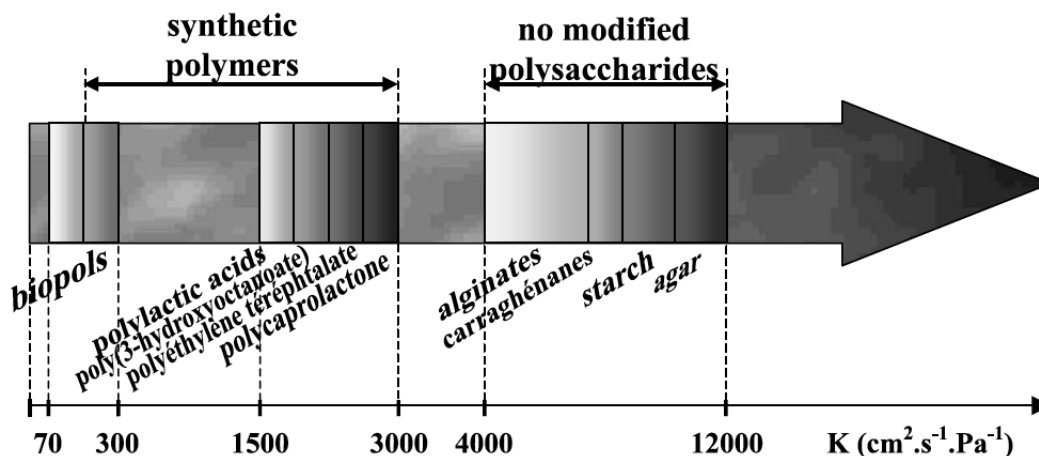


Figure 1.2: Classification of polymers from [Devassine et al. \(2002\)](#).

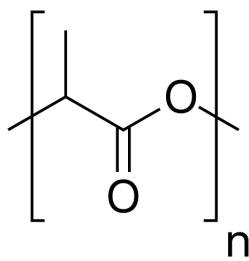


Figure 1.3: Repeating unit of poly(lactic acid).

In other words, it is valuable to investigate lignin modifications and use it to coat urea together with PLA in order to evaluate lignin's potential in commercial development of slow-released fertilizers.

Poly(lactic acid)

Poly(lactic acid) (PLA) is an aliphatic polyester which has been most widely used nowadays as a biodegradable material. It is derived from crops such as corn starch and sugarcane, and is usually produced by direct condensation reaction of lactic acid monomers or the ring-opening reaction of lactide using catalysts (Figure 1.3). Similar to other non-degradable polymers, the properties of PLA material depend highly on the molecular weight, crystallinity and different conformations of the repeating units. It has a relatively high melting temperature e.g. 175-178°C, depending on the crystallinity ([Södergård and Stolt \(2010\)](#)).

As mentioned in section 1.1.1, PLA has superior properties as coating material for fertiliz-

ers. PLA has been used in the fertilizer coating process by blending with other polymers such as polybutylene succinate (PBS) at a high temperature using coating pan (Jompang et al. (2013)). The results showed that the final material was less brittle with higher crystallinity than using PLA alone. However, both the high temperature and complicated equipment cause potential problems when applying the technique in industry. It is considered by us that an alternative way can be to dissolve PLA in solutions, followed by dip-coating process. Therefore, it is important to understand how different organic solvents work on PLA and how the evaporation of organic solvent influences the crystallinity of PLA structure. Effects of 60 different organic solvents on PLA have been analyzed by Sato et al. (2013) using the Hansen solubility parameter (HSP). The conclusion was that aprotic polar solvents are suitable for dissolving PLA. In detail, ether solvents such as 1,4-dioxane, tetrahydrofuran, chlorinated solvent such as dichloroform and chloroform, ketone such as acetone and a few of nitrogen-containing solvent such as acetonitrile are good solvents for the PLA.

While the PLA can be dissolved in the above mentioned solvents, in practice, whether these organic solvents are suitable for PLA polymers by dip-coating process, is still a problem. The evaporating rate of the solvents, dissolving conditions, and final solution concentration of PLA will all influence the final coating film properties. Thus, behaviors of PLA after different dissolution conditions need to be further analyzed, and it will be a part of the present study.

1.2 Lignin

1.2.1 Native lignin

Lignin, as a class of complex aromatic polymers (Lebo et al. (2001)), is a main component in vascular plants. It plays a significant structural role in support tissues in plants. It also helps with the formation of cell walls and protecting wood from fungi attacks.

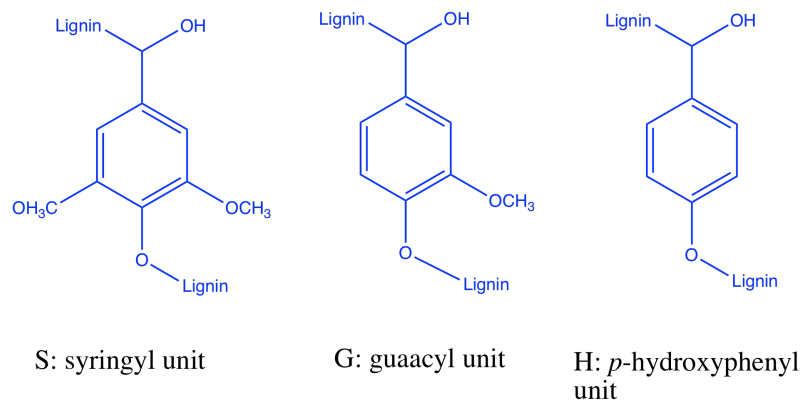
The history of lignin can be traced back to long time ago, when the Swiss botanist first mentioned it as a tasteless and insoluble-in-water material in one of his journals (de Candolle and de Candolle (1844)). Now it is considered as one of the most outstanding bio-fuels, due to its potential availability in large volumes in the world. It also has higher energy efficiency when

compared with other bio-materials such as cellulose. Lignin is practically present in the cooking liquors produced in the pulp and paper industry such as black liquor. Before extracting lignin from the black liquor, for years people used the black liquor for recovering the cooking chemicals as well as producing energy in the mill. In order to extract high quality lignin from black liquor, an unique technology called LignoBoost process was developed by Chalmers university of Technology and the company INNVENTIA (now Research Institutes of Sweden (RISE) /Bioeconomy) at the end of the 1990s. The LignoBoost process makes it possible to maximize the use of lignin and the capacity of the paper industry with relatively low costs.

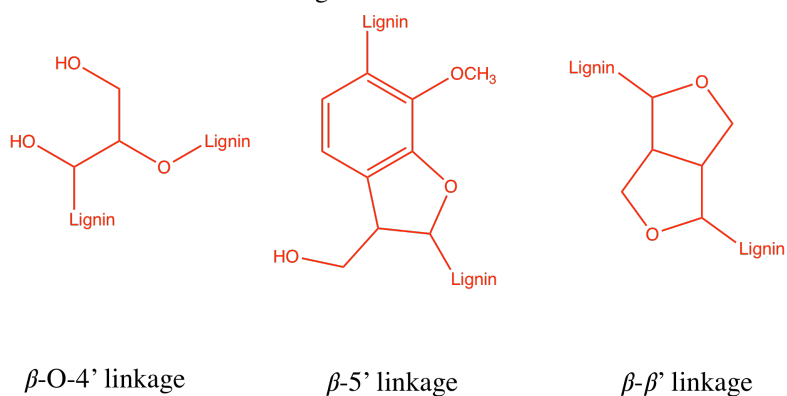
As a biopolymer, lignin is different from most of the other biopolymers because of its heterogeneity. There is still no accurate structural description that can well define lignin. In general, lignin is believed as a cross-linked three-dimensional amorphous structure with molecular weight of more than 7000 g/mol ([Chakar and Ragauskas \(2004\)](#)). However, thanks to the improvement in spectroscopic methods and the efforts of many scientists, many structural features in lignin have been elucidated. It is now known that lignins are built up from phenylpropanes including *p*-hydroxyphenyl- (H), guaiacyl- (G), and syringyl- (S) type aromatic moieties with more than 12 different kinds of linkages between these phenylpropanes ([Liitiä et al. \(2003\)](#)). Lignin structures are also slightly different from each other depend on plant species; softwood lignin has different structures and linkage abundances compared with hardwood lignin. General aromatic ring units, the most common unit linkages and common functional groups in lignin are depicted in Figure 1.4 and detail data could be found in [Sjostrom \(1981\)](#), [Sarkanen and Ludwig \(1971\)](#) and [Karhunen et al. \(1995\)](#), [Karhunen et al. \(1999\)](#)'s articles. The most dominated linkage in softwood lignin is the $\beta - O - 4'$ linkage. With the developing and industrializing of the LignoBoost process, lignins with good quality have become much easier to extract. Many applications have been invented by modifying the structure of lignin. It was considered that domain guaiacyl- (G) units at the C₅ position can be an attractive active sites of modifications for the industrial softwood kraft lignin (SKL), which is used most commonly produced recently from LignoBoost process.

In the N-fertilizers field, lignin has also been proved to be an effective nitrification inhibitor ([Peng et al. \(2004\)](#)), as well as working against urea hydrolysis. The effectiveness is markedly affected by different soil type and temperature ([Yi-zongi et al.](#)). [Lodhi and Killingbeck \(1980\)](#)

Basic units:



Most common inter-unit linkages:



Functional groups: - CHO, - COOH, - OCH₃, - OH...

Figure 1.4: Main structural units, linkages and functional groups, cited from [Mainka et al. \(2015\)](#).

mention that the microorganisms which are responsible for nitrate formation can be restrained by plant-produced chemicals with polyphenolic functional groups, which are largely exist in lignin structure.

1.2.2 LignoBoost process

As mentioned in Section 1.2.1, the LignoBoost process has been working as a successful kraft lignin-sourcing process from black liquor in kraft pulping process in several companies.

An earlier process of extracting lignin from black liquor has severe problems of precipitation. The filter medium is easy to plug with filter cakes and this leads to a low level of washing liquor

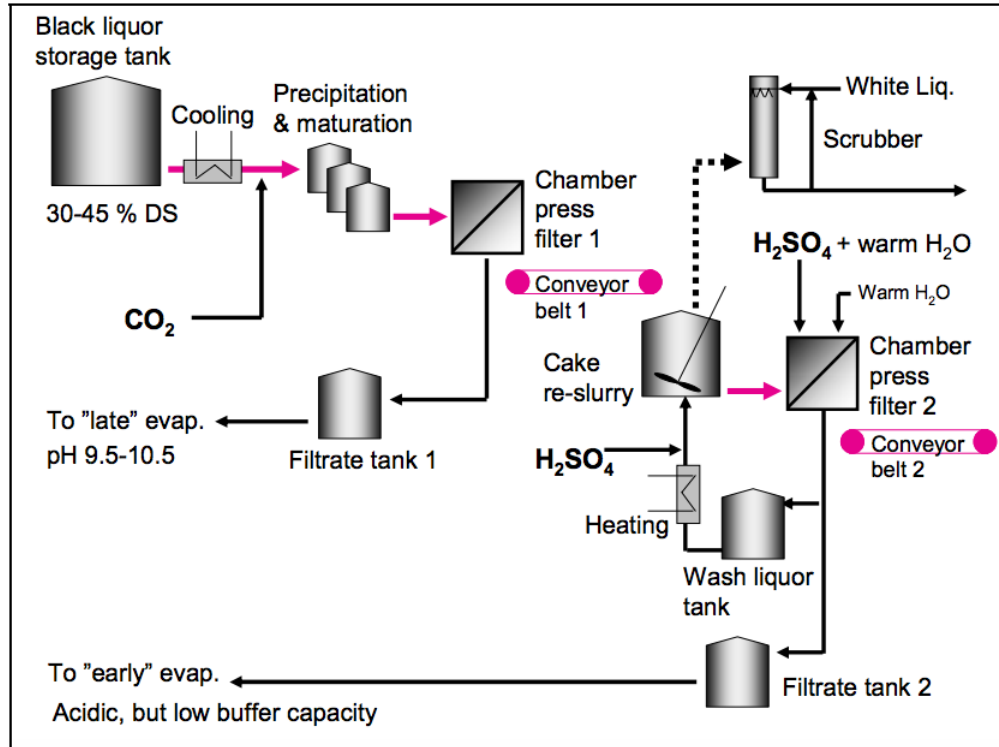


Figure 1.5: General layout of the LignoBoost lignin removal process cited from [Tomani \(2010\)](#).

flowing through the cake. In addition, partial plugging of the filter cake may further cause high impurities level in lignin products ([Tomani \(2010\)](#)). It has been pointed out that these problems are mainly due to the changes of lignin solubility during the process, which is influenced by the pH level and ionic strength in the filter cake during washing process.

In the LignoBoost process, as depicted in Figure 1.5, a flow of black liquor is taken from the storage tank and the lignin inside the black liquor is precipitated by acidification (CO_2) and then filtered. Instead of washing directly after filtration as in the earlier method, the filter cake is delivered with conveyor (belt 1 in Figure 1.5) and goes into the "Cake re-slurry" step. The lignin cake is re-dispersed and acidified here, then delivered into the washing step, "chamber press filter 2". Since the filter cake is re-dispersed in a liquid with low pH and similar condition as the one in the washing step, the changes of pH and ionic strength in lignin will happen in the re-slurry step instead. This prevents the formation of filter cake, differently from the traditional process, therefore gives us a new way in increasing the efficiency and the quality of lignin extraction. With the LignoBoost process, the average dry solid content of lignin can be approximately 63% according to [Tomani \(2010\)](#). [Wang et al. \(2017\)](#) mention that the industrial softwood kraft

lignin (SKL) from this process is of high purity with 99.7 % lignin and 0.35 % of ash. The molecular mass distribution is around 5500 g/mol and the polydispersity index (PDI) is 3.9. With its good properties in many aspects, the industrial SKL from LignoBoost process has been chosen for investigation of many researchers, including coating fertilizers with different approaches.

1.2.3 The Mannich reaction

The Mannich reaction is an organic reaction which has been gradually developing since the 20th century. It is an attractive reaction that has massive value in medicine and bio-synthetic pathways and it is named after a German chemist called Carl Mannich. Normally, the Mannich reaction consists of three components: a primary or secondary amine or ammonia, a nonenolizable aldehyde, and an enolizable carbonyl compound that affords aminomethylated products. During the reaction, it is generally believed that the primary or secondary amines or ammonia are first responsible for the activation of the formaldehyde. The formed imminium ion is attacked by the enol form of the carbonyl functional group. Detailed mechanism of a symmetric Mannich reaction is shown in Figure 1.6, 1.7 and 1.8 (all the figures are cited from TommyCP (2008)).

Nowadays, the Mannich reaction is widely used in lignin to increase the nitrogen content. It is usually conducted with the usage of dioxane, diethylamine and formaldehyde. The reaction happens mostly in the vacant *ortho* position of the phenolic groups of lignin by introducing an aminomethyl group. Since the only vacant *ortho* position in the phenol unit is in the guaiacyl unit (G-unit), the reaction can happen mostly on the softwood lignin, due to its higher content of G-unit than hardwood lignin.

It has been proved that the Mannich reaction with diethylamine can increase the dispersibility of softwood lignin and its usage in fertilizer coating material by introducing organically bound N on the lignin structure (Du et al. (2014)). According to the mechanism of the Mannich reaction, there should also be some other chemicals with similar structures as diethylamine that can be candidates of the reaction. It is worth expecting that these new candidates may give lignin some other valuable characteristic and applications.

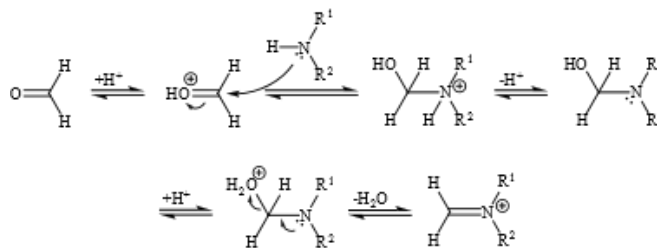


Figure 1.6: The first step of the Mannich reaction: Amine is reacted with formaldehyde to form an iminium ion.

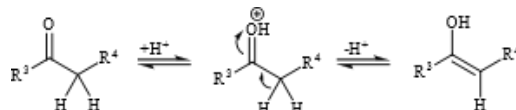


Figure 1.7: The second step of the Mannich reaction: keto-enol tautomerism.

1.3 Lignin-modified slow-released fertilizers

As mentioned in Section 1.1.1 and Section 1.2.3, lignin has been chosen as fertilizer coating material mainly because of its abundance in nature, low costs, and nitrification inhibitory property.

In the past, lignin was directly used without any modification. [Mulder et al. \(2011\)](#) firstly used a pan coater to directly apply dispersion of lignin with 25 % dry matter on urea granules and characterized the coated urea with refractive index meter. However, the results showed that even though these lignin based urea granules have lower release speed compared with the uncoated urea granules, it still cannot reach the requirement of the slow-released fertilizer. After that, in order to improve the coating quality and block deficiencies of single-layered lignin coating fertilizers, lignin was first mixed with melted urea at temperature between 70 to 170°C ([Brücher \(2010\)](#)). The reacted mixture was formed as granules and then coated with resin acid and lignin as coating layers. The resulting lignin urea fertilizer was proved to have great properties as slow-released fertilizers.

Except for mixing urea with lignin and coating with double layers, the chemical structure of

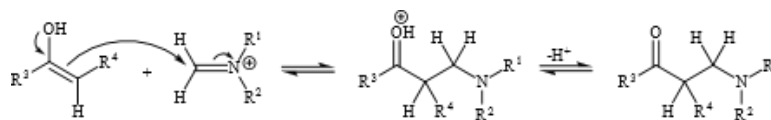


Figure 1.8: The last step of the Mannich reaction: The formed iminium ion is attacked by the enol form of the carbonyl functional group.

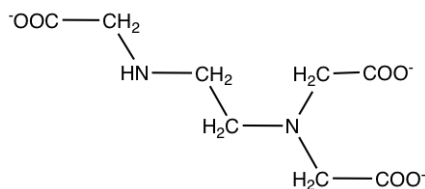


Figure 1.9: The structure of ED3A in its ionic state.

lignin are also modified to meet the requirements of slow-released fertilizers. One way is to process lignin into organically bound N structure in order to make lignin becoming slow-released fertilizer by itself, for example, with the Mannich reaction. Wang et al. (2017) have mentioned that the Mannich reaction of lignin with diethylamine has been used to introduce organically bound nitrogen structure on lignin. It was concluded that the Mannich reaction is best completed when pH = 7 is used. The final product has been grafted with N contained structure successfully. Another method to modify lignin is using some anhydrides. Mulder et al. (2011) have applied alkenyl succinic anhydride (ASA) to increase the softwood lignin's hydrophobicity. The reaction reduced the water-sensitivity of the lignin coating layer. The reactions between lignin and many other anhydrides have also been conducted. It is likely that many anhydrides have the ability to modify lignin to change its water barrier property. However, there is still no relevant articles which give system and detailed data and comparison.

There are still many new developing directions that can boost the potential of lignin in terms of fertilizers, both in modification of lignin structure and the combination with some other polymers.

Ethylenediaminetriacetic acid (ED3A) is a chelating surfactant with low toxicity, high tolerance of salinity and high hard water-resistancy (structure shown in Figure 1.9). It is a derivative from ethylenediaminetetraacetic acid (EDTA), with two nitrogen atoms in each molecule. Compared with diethylamine, ED3A has a similar structure with one hydrogen attached to the nitrogen atom, which makes it chemically favourable and simple for the Mannich reaction. Other than this, it also has an outstanding effect in lowering the surface tension, as well as acting as a metal-chelating structure. This property allows it to be further used in the coating layer for fertilizer to add some micro-nutrients in the soil. It can be an effective chemical to get desired nitrogen containing structure on SKL. Nowadays, there are few synthesis methods of ED3A used commonly in the world. The only commercialized one is from Parker and Cullen (1994), who

invented a process using lauroyl chloride and trisodium salt of ethylenediaminetriacetic acid as raw materials to produce ED3A in large scale. However, this process has high requirements on equipment due to the usage of toxic chemicals. It leads to a relatively high costs, which hinders it to be used in the fertilizer industry. In 2010, [Qiongxin Liu \(2010\)](#) invented a new way of ED3A synthesis with the usage of titanium tetrachloride (TiCl_4), ethylenediaminetetraacetic acid (EDTA) and one oxidant. The method uses more environmentally friendly and low-priced raw materials in the experiment following an easier synthesis process. This method can be an effective and easy way to produce ED3A compound.

However, even though the structure of ED3A is similar to diethylamine, whether the Mannich reaction between lignin and ED3A can be conducted smoothly or not is still unknown. Experimental test is needed.

1.4 Characterization methods

1.4.1 NMR spectroscopy

Nuclear magnetic resonance (NMR) spectroscopy is a technique that is usually used in chemical or physical research to determine the chemical structures from different atoms present in the structures. The results of NMR spectroscopy can supply information about changes and completion extents of lignin modifications. Here is the basic of nuclear magnetic resonance: each nuclei in a magnetic field absorbs and re-emit electromagnetic radiation ([Shah et al. \(2006\)](#)). When adding a specific strength of magnetic field, the resonant frequency, the energy of absorption and the signal of each atoms are generally unique. However, the intramolecular magnetic field around, an individual atom in the molecule also changes the resonance frequency and will lead to a shift of residual peak in the final signal. Therefore, after analyzing the signal that the NMR spectroscopy provides, different functional groups are distinguishable and easy to analyze. To obtain NMR signals, the sample is commonly dissolved in a solvent and if running on solid sample, another special process called magic angle spinning (MAS) is needed.

A NMR machine usually consists of a strong magnet which has a space inside to hold and spin the samples, a radio frequency emitter and a probe which usually stays inside the magnet,

that can receive the energy. The spinning of the samples is to average the diffusional motion (Johnson (1999)). Samples are prepared by adding deuterated solvent such as deuteriochloroform (CDCl_3) since the majority of nuclei in a solution is solvent and will mostly contain NMR reactive protons. The chemical shifting for different solvents have little differences and the NMR spectroscopy can be calibrated according to the known solvent proton peak.

In the NMR spectroscopy, the chemical shifting is the foundation of analyzing different chemical structures and is due to variations of nuclear magnetic resonance frequencies of the same kind of nucleus in different electron distributions. Chemical shift is represented by parts per million (ppm) of frequency. The calculating equation is as follow (Harris et al. (2001)):

$$\delta = \frac{\nu_{sample} - \nu_{ref}}{\nu_{ref}} \quad (1.1)$$

where ν_{ref} is the absolute resonance frequency of a standard reference and ν_{sample} is the absolute resonance frequency of the sample atom when the magnetic field is the same. It is worth mentioning that the chemical shift is independent of magnetic field strength, whereas the absolute resonance frequency increases with the ascending magnetic field strength.

By reading the chemical shift got from the data compared with the internal standard, different structures can be interpreted by using a specific software such as 'MestReNova'. The shape and the area of the peaks can be an indication of chemical structures. By doing integration of the peak area, the ratio of same protons in different functional groups can be obtained. However, this principle is only accurate in the simplest one dimension ^1H NMR tests. When it comes to the ^{13}C NMR spectra, the integral of the peaks depends also on other factors like dipolar coupling constants which are difficult to measure. So the integral of these NMR spectra can not always provide enough quantitative information.

J-coupling is a phenomena that shows the most information in the one dimension NMR spectrum. It is due to the interaction between two nuclear spins, which, in the NMR spectra, shows in the manner of multiple peaks of signals for simple molecules. The spin-spin interaction of different molecules in different spin states through chemical bonds leads to the splitting of signals (Hahn and Maxwell (1952)). For spin 1/2, the coupling of n equivalent nuclei will split the peak into $n + 1$ multiple peaks. And the splitting rules follow the Pascal's triangle as seen in

Table 1.1: The Pascal's triangle.

Multiplicity	intensity ratio of the peaks
singlets	1
doublet	1:1
triplet	1:2:1
⋮	⋮

Table 1.1. For a spin 1 nucleus, the pattern of splitting follows another rule into 1:1:1 because a spin 1 nucleus has three spin states.

J-coupling and chemical shifting give chemists detailed information of structures of chemicals, environments of nucleus and linkages between molecules. Depending on the different internal standard, different atoms such as H, C and P can be analyzed.

³¹P NMR analysis

The hydroxyl groups of modified lignin structures are mostly analyzed by using ³¹P NMR. In the work by [Granata and Argyropoulos \(1995\)](#), the ³¹P NMR analysis of the functional group distribution in lignin has been thoroughly examined by using 2-chloro-4,4,5,5-tetramethyl-1,3,2-dioxaphospholane as a phosphorylation reagent. The amount of the hydroxyl groups are related to the hydrophobicity of the final lignin samples. Therefore, it is a good characterizing method when the aim the research is to evaluate the hydrophobicity and quantify the hydroxyl groups of the modified lignin sample and their products.

¹³C NMR analysis

The ¹³C NMR is an effective way of investigating carbon structure in the organic compounds. With the usage of some organic solvents (in this study commonly DMSO), one can test the net spin of ¹³C atoms and identify carbon atoms in the organics by reading the chemical shifts of carbon atoms. It is worth noticing that even though the chemical shifts are caused by following the same mechanism as proton NMR, the chemical shift values in the ¹³C NMR spectra are much larger than the value in ¹H NMR spectra.

Other than this, the sensitivity of the ¹³C NMR spectra is much less than the ¹H NMR spectra, mainly caused by the major isotope of ¹²C. Since the ¹²C has a spin quantum number of

zero, which is not magnetically active, it causes decreases of sensitivity. However, by adding the relaxation agent (for example, chromium(III) acetylacetonate), the testing time can be reduced into a reasonable range, so that more scans can be made to obtain higher signal/noise ratio.

2D HSQC NMR analysis

2D NMR (most of the case as heteronuclear single-quantum correlation spectroscopy (HSQC)), is also widely used in the lignin structure determination. 2D HSQC NMR detects correlations between two different types of nuclei which are linked together by one bond. This test gives a figure with peaks, which is the combination of two connected atoms shifts at the same time. Therefore, it is a good characterization method for testing changes of, for example, C-H linkages due to chemical reactions in lignin structures.

1.4.2 Contact angle test

Contact angle test is a common way to get wettability information of a solid surface. It has been used in many industry, such as oil and lubricant. It has also been used in the hydrophobicity tests of different polymer films. Measurements of contact angles are usually considered as the primary step of studying wettability when a solid and liquid contact. Small contact angle ($\ll 90^\circ$) corresponding to high wettability while the one higher than 90° corresponding to low wettability. The three-phase contact of solid, liquid and vapor is described with the well-known Young equation (Equation 1.2):

$$\gamma_{LG} \cos \theta_C = \gamma_{SG} - \gamma_{SL} \quad (1.2)$$

where γ_{SL} , γ_{SG} , and γ_{LG} represent the solid-liquid, solid-vapor, and liquid-vapor interfacial tensions, respectively (Figure 1.10). θ_C is the Young's contact angle. The Young equation assumes that the surface of the solid is ideally homogeneous. However, due to the imperfection of the surface at most of the cases, the contact angle value shows variations from the real contact angle.

Actually, on an ideal surface, the Young equation works well and the final contact angle getting from experiment is equal to the real contact angle. However, for a real surface with unevenness structure, the liquid-vapor interface and the actual surface of the solid are not the same.

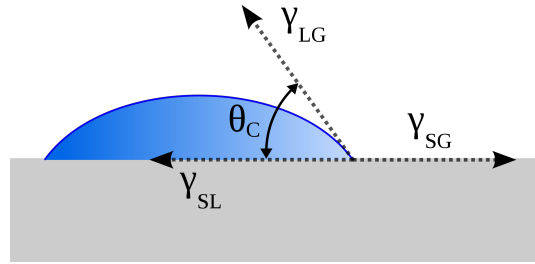


Figure 1.10: Schematic diagram of a Michelson interferometer, configured for FTIR, cited from [Sanchonx \(2011\)](#).

The real contact angle should be the tangent value of these two surfaces. And the toughness of the solid surface should be considered when judging the wettability according to the contact angle. In 1936, Wenzel has defined the relationship between roughness and wettability in a real surface ([Wenzel \(1936\)](#)):

$$\cos \theta_m = r \cos \theta_C \quad (1.3)$$

where θ_m is the measured contact angle, θ_C is the Young contact angle and r is the roughness ratio. The roughness ratio is 1 for an ideal surface and >1 for rough surface. This equation only applies when the scale of droplets is 2 to 3 order of magnitude larger than the roughness scale.

According to the equations, higher surface roughness will enhance the wettability when the other parameters remain the same.

1.4.3 SEM spectroscopy

Scanning electron microscope (SEM) works with a beam of focused electrons. By scanning the electrons on the surface of objects and getting the emitting secondary electrons, images contain information of the surfaces will be obtained after the secondary electrons are collected from the surface within a really small distance. Therefore, high-resolution images of a sample surface can be captured using SEM (less than 1 nm). The samples put in the SEM equipment need to fulfill the requirements of testing. In most of the cases, the sample needs to withstand high energy beam of electrons, as well as the vacuum conditions (dry sample). The size should be small enough to put on the testing stage. And it needs to be electrically conductive. Some SEM equipment requires a thin coating layer of metal for the nonconducting samples. But in some

cases, the sample can be put directly without coating, such as for the so called environmental SEM (ESEM) or low-voltage mode of SEM operation.

Due to its special principle, SEM does not need objective lenses to magnify the objective. The magnification of SEM can be about 6 orders of magnitude from about 10 to 500,000 times. It can also be used to observe the three-dimensional appearance of the samples. Many researches use it as a tool for measurement in the nano-scale. It is also an effective method to test the surface roughness conditions.

1.4.4 FTIR spectroscopy

Fourier transform infrared spectroscopy (FTIR) is a technique widely used in chemistry field to get the infrared spectrum of absorption of a subject in its solid, liquid and gas states. By measuring the degree of absorbing light of the sample at each wavelength, one can get detailed structure information of the testing sample. The mechanism of the FTIR spectroscopy is by shining beams containing many frequencies of light on the sample for a few times (changing frequencies at each time) and measuring the absorption of lights by the sample every time using computer, to obtain the absorption at each wavelength at the end.

An important part of FTIR spectroscopy equipment is the Michelson interferometer, as seen in Figure 1.11. Light resources from a radiator are collimated and shot towards a beam splitter. According to the refraction and transmission rules, around 50 % of the light is refracted on to the stationary mirror and 50 % of the light goes onto the moving mirror. These two light beams refracted back from mirrors and go through the beam splitter. The recombined beam goes directly on the sample and, through the sample, goes on the detector. Due to the difference between two optical path length, the optical path difference (OPD) is obtained. And by varying the position of the moving mirror, in other words, by changing the optical path difference, the detector can record the data and get the interferogram results. By analyzing the interferogram difference between background (no samples) and when the sample presents, the absorption bands of the sample can be collected and the data can be further used in the chemical researches.

FTIR has been widely used in the field of organic chemistry and many researches has been conducted about characteristic vibrations of various functional groups. For example, the stretching and bending modes of the O-H and C-O moieties are the characteristic vibrations of the

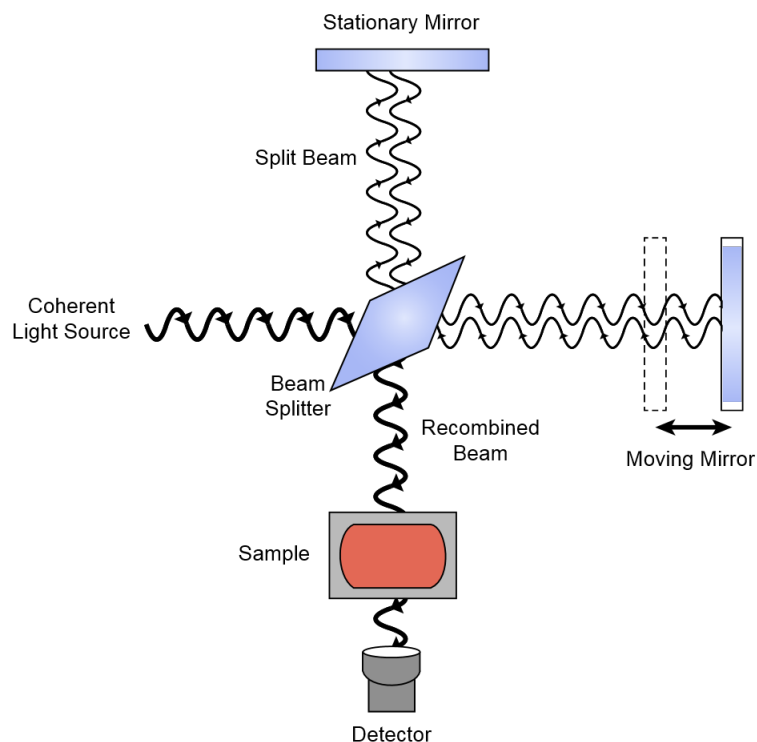


Figure 1.11: Schematic diagram of a Michelson interferometer, configured for FTIR, cited from [Sanchonx \(2011\)](#).

O-H grouping. Many books have comprehensive records of the group frequencies for many structures such as phenols and alcohols. In the field of lignin chemistry, FTIR is usually used to characterize the differences of lignin structures. By comparing the FTIR figures, such as the moving of peaks, one can estimate the extent of different modification reactions.

1.5 Objectives

Lignin, as a biodegradable material, is an attractive candidate of coating material in slow-released fertilizers. However, the single layer lignin does not show favorable performance in slowing down the releasing rates of fertilizers. Investigations on the lignin modifications with esterification reactions and the Mannich reactions, and its combination methods with PLA still need to be continued on the slow-released fertilizers. NMR spectroscopy and FTIR spectroscopy should be used to analyze the samples. Furthermore, the properties of PLA/lignin complex need to be determined. The wettability of the final films should be tested by contact angle tests and observed by SEM spectroscopy. The dip-coating techniques need to be combined with properties

of coating materials (in this case PLA/lignin complex), and at the end come up with a more economically feasible and practical solution. The final urea pellets properties needs to be detected and compared, too.

The main objectives of this Master's project are

1. Conducting and analyzing derivatization reactions on the lignin (SKL) structure by using different chemicals in order to change the hydrophobicity (esterification reaction) and increase the N value (the Mannich reaction by diethylamine) of lignin samples.
2. Synthesizing ED3A compound with an environmentally friendly method in order to use it in the Mannich reaction. Grafting the ED3A compound on the lignin structure to increase the N value and potentially become a chelating agent of metal, so as to add essential trace elements into the final fertilizer products.
3. Finding good solutions of mixing modified lignins with PLA as composite coating materials. And using it as a coating layer for urea fertilizer. Investigating the effects of PLA/modified lignin on the urea releasing speed.

Chapter 2

Experimental

2.1 Chemicals and materials

All water used in this experiment as solvents or reagents was Milli-Q water (resistivity 18.2 M Ω -cm at 25°C). The softwood kraft lignin (SKL) used was prepared following the LignoBoost process mentioned above from the black liquor obtained from industrial kraft pulping of softwood. SKL was directly used without further refining. It has a high purity with 99.7 % lignin with a low content of ash (0.35 %) and carbohydrates (1.2 %). The molecular mass distribution (MMD) value is 5500 g/mol (Mw) and the polydispersity index (PDI) is 3.9. Detailed structure characteristics results can be found in [Wang et al. \(2017\)](#). Urea pellets, palmitic anhydride (90-95 %), lauric anhydride, and ethylenediaminetetraacetic acid (EDTA) were purchased from Sigma Aldrich. Poly(lactic acid) (PLA, PL80) was obtained from Unitika Ltd. (Osaka, Japan). Its molecular weight is around 140567 g/mol. Pyridine used as solvent of derivative reactions, diethamine, dioxane, formaldehyde solution (min. 37 %), ammonium hydroxide (25 %), trifluoroacetic anhydride (TFAA), acetic anhydride, dichloromethane (DCM), tetrahydrofuran (THF) and acetone were purchased from Merck Millipore (Merck KGaA, Germany) while methanol was purchased from Honeywell International Inc.

2.2 Esterification of lignin

In order to improve the water barrier properties of the final coating layer, SKL, as the main investigated structure, was modified by the esterification reactions.

As described in Section 1.4.1, several acid anhydrides, such as alkenyl succinic anhydride (ASA) have been found having the ability to change the lignin structure to make it more hydrophobic by esterification reactions. In this study, acetic anhydride, palmitic anhydride and two other anhydrides: lauric anhydride and trifluoroacetic anhydride were chosen to modify SKL structure. The final products were analyzed using different characterization equipment to study their structures/properties. With the addition of pyridine as solvent and catalyst, the following general procedures (adapted from acetylation) were proceeded as described in [Gellerstedt \(1992\)](#). All the softwood kraft lignin (SKL) used in this experiment was freeze dried to remove the water in the sample before certificate, so the dry content of SKL is 100 %.

Briefly, the reaction between Ac_2O and SKL was conducted by adding 5 ml acetic anhydride (Ac_2O)/pyridine (1:1, v:v) mixed solution onto 500 mg SKL and stirring at room temperature for 24 h. After the reaction, water and methanol were added to decompose the excess anhydride reagent. Then the mixture solution was evaporated under reduced pressure until dryness. After that the residue was suspended in toluene and evaporated (repeating for three times) in order to remove the acetic acid formed. At the end, the remained toluene in the mixture was removed by addition of methanol and evaporation (this method can maintain the complete recovery of lignin sample with the least impurities additions). The final lignin derivative is denoted as AcSKL in this report.

The palmitoylation of SKL was proceeded by using 400 mg SKL (approximately 2 mmol of lignin aromatic units considering the molecular weight as 200 g/mol), with the adding of 8 mmol palmitic anhydride and 5 ml pyridine and reacted at room temperature for 24 h. After the reaction, the mixture was refluxed under 70°C for 1 h. Excess anhydride reagent was decomposed by addition of water and methanol. After filtration and washing with water until neutral pH, the final sample was freeze-dried over night to remove all the water. The final lignin derivative is denoted by PaSKL here.

The reaction between trifluoroacetic anhydride (TFAA) and SKL was conducted in a similar

manner as the reaction with palmitic anhydride: SKL and TFAA were added with a mole ratio of 1:5 (1 mmol: 5 mmol) in 5 ml pyridine solution at room temperature for 24 h, followed by refluxing for two hours under 70°C (considering the potential steric hindrance of TFA). Excess anhydride reagent was decomposed by water and methanol, followed by washing with water until neutral pH and freeze drying. The final lignin derivative is represented by TFASKL.

2.3 The Mannich reaction

In addition to the esterification reactions mentioned above, another reaction, the Mannich reaction, was also conducted in this study. The Mannich reaction, using diethylamine as reactant, was commonly applied on the lignin when it comes to the modification of lignin. The aim of this reaction is to add organically bound N onto lignin structure. It gives a chance for lignin derivatives to become N carriers so that they can offer N in slow speeds from the fertilizer coating layer.

2.3.1 Reaction between diethylamine and lignin

The first Mannich reaction was conducted with diethylamine as reactant with the method mentioned in [Wang et al. \(2017\)](#). 500 mg SKL (around 2.5 mmol) was first dissolved in 5.0 ml dioxane, then mixed with 27.5 mmol diethylamine and 27.5 mmol formaldehyde at pH =7. The mixture was put in a sealed bottle and stirred for 4 h at 60°C. Since the excess reagents were all volatile chemicals, the final mixture was put under freeze drying machine over night until all the solution and excess reagents were removed. The final lignin derivative is denoted as ManSKL.

2.3.2 Reaction between ED3A and lignin

Instead of the original diethylamine, another chemical, ethylenediaminetriacetic acid (ED3A), was also tried in this study to introduce desired nitrogen containing structure on SKL.

Synthesis of ED3A

In order to obtain the ethylenediaminetriacetic acid (ED3A), which is not commercially available, following steps were conducted in this study: 1). First of all, EDTA (20 mmol) was dissolved in 20 ml Milli-Q water, following by the addition of ammonium hydroxide ($\text{NH}_3 \cdot \text{H}_2\text{O}$) until $\text{pH}=7$. Then TiCl_4 (20 mmol) was added in the solution drop by drop. After that $\text{NH}_3 \cdot \text{H}_2\text{O}$ was added slowly until the pH was adjusted to 3.0. The mixture was placed at room temperature for 0.5 h until the reaction was completed. The resulting white 'micro-crystal' powder was filtrated out and air-dried at room temperature. 2). The synthesized white powder was taken out and dissolved in 5 ml water, followed by 30 % H_2O_2 dropping in with constantly stirring. $\text{NH}_3 \cdot \text{H}_2\text{O}$ was added again to adjust the pH to 2. After that, the solution was placed at 25°C water bath for 24 h and evaporated at room temperature with reduced pressure until some yellow precipitate came out at the bottom. The yellow precipitate was then collected by centrifuging the concentrated solution and air-dried at room temperature for two days. 3). The dried yellow precipitant was weighed and dissolved in 5 ml water and the pH was adjusted to 8 with $\text{NH}_3 \cdot \text{H}_2\text{O}$. The solution was placed in the oil bath at 80°C and reacted for 24 h. 4). 5 M NaOH was added in the above solution until the pH reached 12. After reacting at 90°C for 5 h, the white SiO_2 precipitant in the solution was filtrated off and the filtrated solution was collected. It was then transferred to a freeze drying machine. The final dry product was analyzed by NMR spectroscopy (H- and C- NMR) and the results showed that the synthesized product contains ED3A (detailed information can be found in Chapter 3).

Reaction between ED3A and vanillyl alcohol

In this experiment, reactions between vanillyl alcohol (model compound of softwood lignin) and ED3A were first conducted to avoid the expected steric hindrance between ED3A and the softwood kraft lignin.

Vanillyl alcohol is chemically derived from vanillin, which is mostly used as a food additive in vanilla cream and other vanilla flavored food. The structure of the vanillyl alcohol is depicted in Figure 2.1. This methoxybenzyl alcohol structure is highly similar to the G-unit, as well as without the steric hindrance as in the lignin structure. Therefore, many researchers used it as

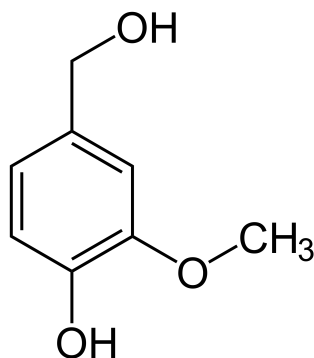


Figure 2.1: The aromatic ring structure of vanillyl alcohol, with a similar structure to the G-unit in softwood lignin.

the lignin model compounds to proceed related experiments so as to understand the reaction without the steric hindrance.

Detailed experiment is as follow: vanillyl alcohol (50 mg, 0.25 mmol) was first mixed with synthesized ED3A and formaldehyde at mole ratio of 1: 2: 2. The mixed solution was then adjusted to pH = 11.5 with 6 M NaOH and put at 90°C oil bath for 3 h, followed by freeze drying. The final product is denoted as ED3AVA in this study.

Reaction between ED3A and lignin

ED3A modified lignin was prepared after a similar procedure, too. The dried SKL(50 mg, 0.25 mmol) was mixed with synthesized ED3A and formaldehyde at mole ratio of 1: 2: 2. And the mixed solution was adjusted to pH = 11.5 with 6 M NaOH and put at 90°C for 3 h, followed by freeze drying. The final product is denoted as ED3ASKL in this study.

2.4 NMR spectroscopy

All the NMR tests were conducted on a Bruker Advance NMR system with UltraShield Plus 400 MHz magnet (Bruker, Bermen, Germany) with a broadband PFG 5 mm probe, and the data were analyzed by the MestReNova 9.0.1 software (Mestrelab research, Santiago de Compostela, Spain).

The OH groups of derivative lignin samples were phosphitylated and quantified by ^{31}P NMR spectroscopy with the use of 2-chloro-4, 4, 5, 5-tetramethyl-1, 3, 2-dioxaphospholane, follow-

ing the method described by [Granata and Argyropoulos \(1995\)](#). 30 mg dried lignin or derived lignin sample was dissolved in 100 μl pyridine/*N,N*-dimethylformamide (1:1), with the addition of internal standard (IS): 100 μl *N*-hydroxy-5-norbornene-2, 3-dicarboxylic acid imide pyridine solution (20 mg/ml) and relaxation agent, 100 μl chromium acetylacetonate pyridine solution (5 mg/ml). Then the reagent, 2-chloro-4, 4, 5, 5-tetramethyl-1, 3, 2-dioxaphospholane, was added and the mixture was stirred with magnetic stirrer for 10 min to accomplish the reaction. Chloroform-*d* (400 μl) was then added as solvent and the whole solution was transferred into sample tube and placed onto the NMR spectroscopy equipment.

The structure of ethylenediaminetetraacetic acid (EDTA) and ethylenediaminetriacetic acid (ED3A) were analyzed by quantitative carbon (^{13}C -NMR) and hydrogen (^1H -NMR) spectroscopy. All the samples were dissolved in Deuterium oxide (D_2O) with two drops of *d*-acetone for signal calibration.

Quantitative carbon (^{13}C -NMR) and hydrogen-carbon 2D heteronuclear single quantum coherence (^1H - ^{13}C 2D HSQC NMR) nuclear magnetic analyses were performed on all the modified lignin samples in order to analyze their structures. All the samples were dissolved in dimethyl sulfoxide-*d*₆ or chloroform-*d* (for PaSKL and LauSKL) depending on the solubility.

2.5 FTIR analysis

The structure of the modified lignin was characterized by attenuated total reflectance-Fourier transform infrared (ATR-FTIR) spectroscopy. The experiments were proceeded with a Perkin-Elmer Spectrum 2000 FTIR spectrometer (Waltham, MA, USA). It was equipped with an ATR system and a Specac MKII Golden Gate (Crecstone Ridge, GA, USA). Spectra were scanned in the range of 4000 to 600 cm^{-1} , in 1 cm^{-1} intervals with 4 cm^{-1} resolution over 16 scans at room temperature. Before testing all the samples, a background scan was conducted to make background correction. Spectra were ATR and baseline corrected. Normalization of the spectra was made with the signal at 1511 cm^{-1} (aromatic skeletal vibration with C=O stretching).

2.6 Film casting

PLA was selected as the basic component for the coating composites with lignin in this study. It has been proved to be an effective biopolymer as a water barrier. Biodegradable films that are completely based on renewable resources can thus be prepared by mixing lignin derivatives with dissolved PLA.

In order to test the characters of coating material and choose better materials combination for film casting, thin films were made with PLA with different concentrations and lignin derivative complex solutions in this study. First, PLA was used as the coating polymer and was dissolved in dichloromethane (DCM) by stirring under room temperature with magnetic stirring for one day at a ratio of 60 %, 30 %, and 15 % (w/v). PLA films were first made by film casting these solutions on Petri-dishes separately. The film with the best performance which is 30 g/100 ml was selected as the final formula for later films and in the coating procedure.

Six lignin solutions were prepared with DCM/THF (v/v: 0:5, 1:4, 2:3, 3:2, 4:1, 5:0) to test the influences of dissolving agents on the final films. In detail, original lignin was first added in DCM/THF mixing solutions with stirring until it dissolved (6 %, 6 g/100 ml for each solution sample). Then the solutions were mixed with PLA/CH₂Cl₂ (30 g/100 ml) by adding lignin containing solutions drop by drop into the PLA solution with magnetic stirring (v/v = 1:1). The final mixtures were directly poured on Teflon Petri-dishes and dried at room temperature for 24 h until they were totally dry. The films' thickness were all around 47-60 μm. All the films were analyzed by contact angle test and SEM observation. Ratio in film with the best performance ($v_{DCM}/v_{THF} = 3:2$) was selected into next steps.

Lignin derivative samples (6 g/100 ml) were dissolved in DCM/THF (v/v = 3/2) solution then mixed with 30 % PLA/DCM with the same way as mentioned above. Final casting films were analyzed by contact angle tests and SEM tests.

2.7 Contact angle tests

A SL 100B contact angle meter from Solon Information Technology Co., Ltd.(Shanghai, China) was used in this study to test the contact angle of different films. All the tests were recorded when the data were stable (approximately 1 min). The pendant drop method was proceeded at

23°C with relative humidity (RH) of 50 %. All the results were collected and compared in chapter 3.

2.8 Scanning electron microscopy (SEM) tests

SEM tests were performed with a HITACHI SU3500 scanning electron microscope. All the samples were directly mounted on the SEM plate for analysis. Final figures can be found in chapter three.

2.9 Urea coating and water immerse tests

Urea pellet was screened by sieves and the ones with diameters of 1-2 mm were selected in the following experiment. Dip-coating was conducted by immersing these urea pellets into the PLA/SKL solution as mentioned for 3 min and then taking out. They were separated and placed on Teflon film, following by air drying for one day. This process was repeated for three times on the urea pellets.

Each pellet was put in a small bottle with 25 ml distilled water after coating. Time was counted at the same time until the coating layer was floated on top of the water. In this study, 50 pellets were tested in total to have a more accurate result.

Chapter 3

Results and discussion

3.1 Lignin modifications

3.1.1 Original SKL lignin

The original SKL lignin used in this study is a typical softwood lignin which have many functional groups. It can be used in several structural modifications.

With the usage of ^{31}P -NMR analysis, all the OH groups in the lignin samples can be phosphorylated and quantified. All the chemical shifts were referenced to the signal of the internal standard ($\delta_{IS} = 151.9$ ppm). The amount of individual OH groups was obtained by the integration of following regions: aliphatic OH: 145.4-150.0 ppm; condensed phenolic OH (including a small quantity of syringyl OH):140.2-145.4 ppm ; guaiacyl phenolic OH: 139.0-140.2 ppm; *p*-hydroxyphenyl phenolic OH: 136.5-138.6 ppm and carboxylic OH: 133.6-136.0 ppm.

In the original lignin samples, as can be seen in the Figure 3.1 (from left to right), there are some aliphatic hydroxyl groups (around 1.91mmol/g) mainly at the C_α and C_γ on its side chain (Figure 3.4 (on the left)), some condensed phenolic units (2.01 mmol/g, which contains some syringyl (S) units), some non-condensed phenolic hydroxyl groups (mostly from G-units, 2.32 mmol/g, followed by H-unit, 0.24 mmol/g), and finally a small amount of carboxylic hydroxyl groups (0.46 mmol/g). (All the results are obtained from duplicated determinations). Detailed calculations are in Appendix A.

Here, all the aliphatic hydroxyl groups (around 1.19 mmol/g) and around 4.6 mmol/g aro-

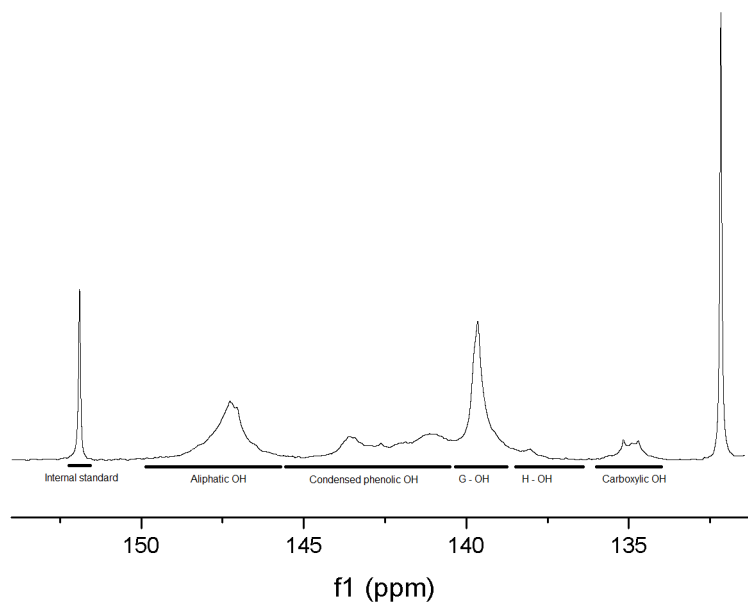


Figure 3.1: The ^{31}P -NMR spectra of original SKL, peaks from left to right: Internal standard, Aliphatic OH, Condensed phenolic OH, G-OH, H-OH, and Carboxylic OH.

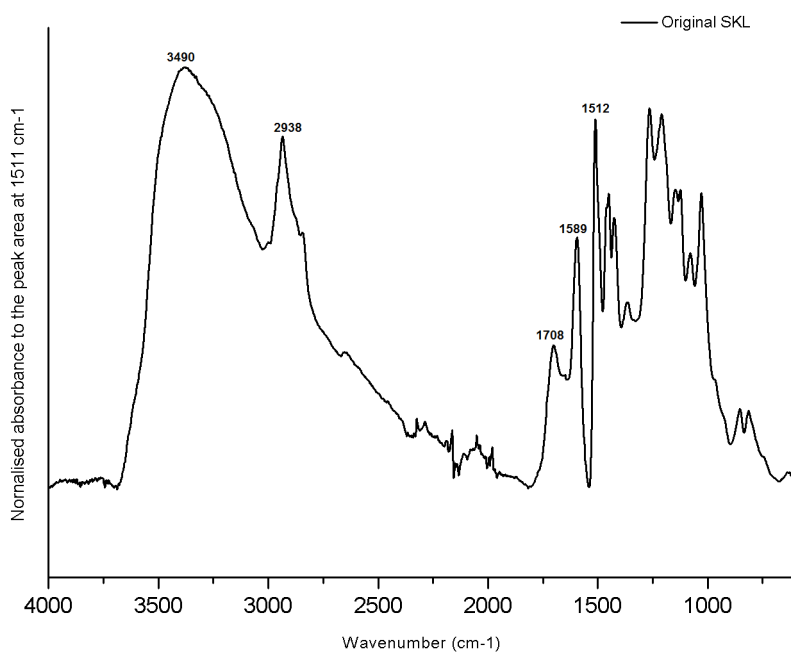


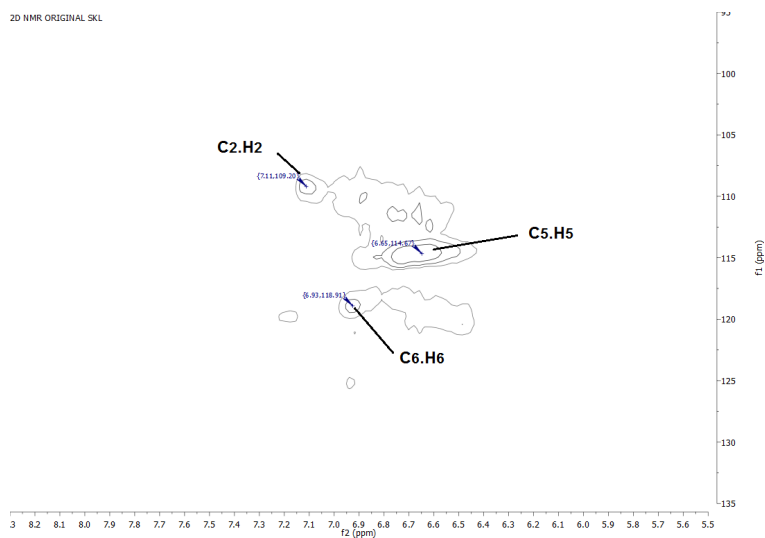
Figure 3.2: FTIR spectroscopy of original SKL sample. Some peak wave-numbers are marked out.

matic hydroxyl groups are susceptible to be modified in the lignin structure.

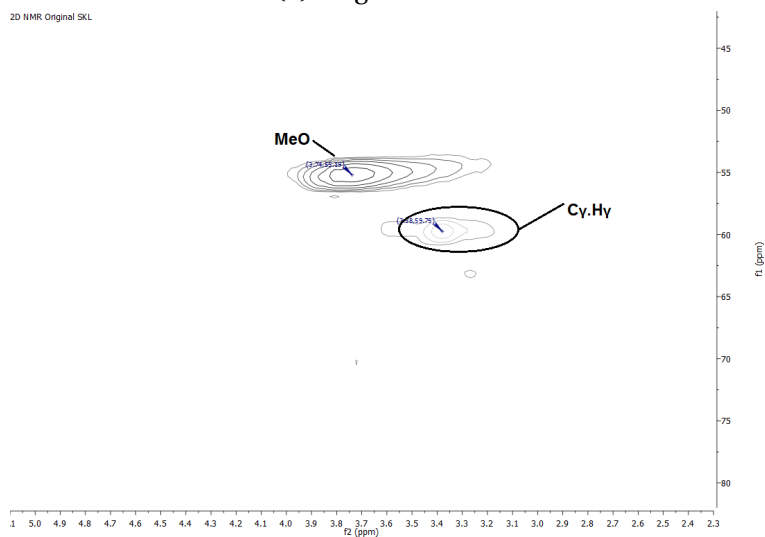
On the other hand, as can be seen in the FTIR spectrum in Figure 3.2, many structures in the original SKL can be identified. According to a number of FTIR reference literature (mainly Socrates (2004)), some of the structures can be interpreted from the peaks in FTIR spectra. At approximately 3300 to 3400 cm^{-1} , the intensity of the FTIR signal has a relatively wide peak. This is the O-H stretching region, which generated from the stretching of H-bonded aliphatic and aromatic hydroxyl groups. The absorption at around 2938 cm^{-1} is mainly due to the C-H stretching in the aliphatic methyl and methylene groups of the side chain. The stretching of C=O causes the appearance of absorption peak at around 1708 cm^{-1} , corresponding to the carbonyl stretching of ester and carboxyl groups in lignin. The existence of C-O structure in lignin gives a peak around 1266 cm^{-1} . As for the peaks at 1589 cm^{-1} , it is related to the aromatic ring breaths with C=O stretching in lignin. The vibrations of aromatic skeleton leads to the peak at 1512 cm^{-1} .

FTIR spectra can also be used for investigations of chemical modifications of these samples. The increase of these peaks might give evidence of acylation modification, as well as amination reactions.

Two-dimensional ^1H - ^{13}C NMR spectra (2D NMR) is able to provide important structural information of lignin samples, too. By comparing the results of HSQC cross-signals of lignin and associated structures with the published literature (Yuan et al. (2011)), many lignin cross-signals in the lignin samples can be assigned accordingly. Since there are many signal peaks present in the 2D NMR spectra of lignin but not all of them are informative, only peaks which may be influenced by the modification reactions are discussed and compared in this study. In detail, the original SKL sample (Figure 3.3a) has three main cross-signals in the aromatic region. They are from aromatic rings of guaiacyl (G) units, which show correlations for C₂-H₂, C₅-H₅, and C₆-H₆ at $\delta_C(ppm)/\delta_H(ppm)$: 109.20/7.11; 114.67/6.65; 118.91/6.93, respectively. Meanwhile, at the side-chain regions (Figure 3.3b), the NMR spectra shows prominent signals corresponding to methoxyls ($\delta_C(ppm)/\delta_H(ppm)$: 55.19/3.74) and C γ -H γ linkages in β -O-4' substructures ($\delta_C(ppm)/\delta_H(ppm)$: 59.75/3.38).



(a) Original SKL A.



(b) Original SKL B.

Figure 3.3: Aromatic (A) and side-chain (B) regions in the 2D HSQC NMR spectra of original SKL used in this study: $\delta_C(ppm)/\delta_H(ppm)$: 97-135/5.5-8.3, and 43-82/2.3-5.1.

3.1.2 Esterifications of lignin

The esterification reactions of SKL were conducted with four different anhydrides. Since the G-unit is the most abundant unit that can be involved in the esterification reactions in lignin structure, the reaction extent of G-unit was analyzed in this study. The possible reactions for the G-units of lignin structure are first shown in Figure 3.4 (top). The aliphatic chains ($R=CH_3$ for acetic anhydride, $R=CH_3(CH_2)_{14}$ for palmitic anhydride, $R=CH_3(CH_2)_{10}$ for lauric anhydride) and the group of trifluorine carbon ($R=CF_3$) may be coupled as the fatty acid esters in the SKL lignin structures with pyridine as catalyst and solvent. The replacement of fat acid into aliphatic chain in the final lignin structures may increase the hydrophobicity of the modified lignin. For the LauSKL and PaSKL, their hydrophobicity are expected to be higher due to the existence of long carbon chain.

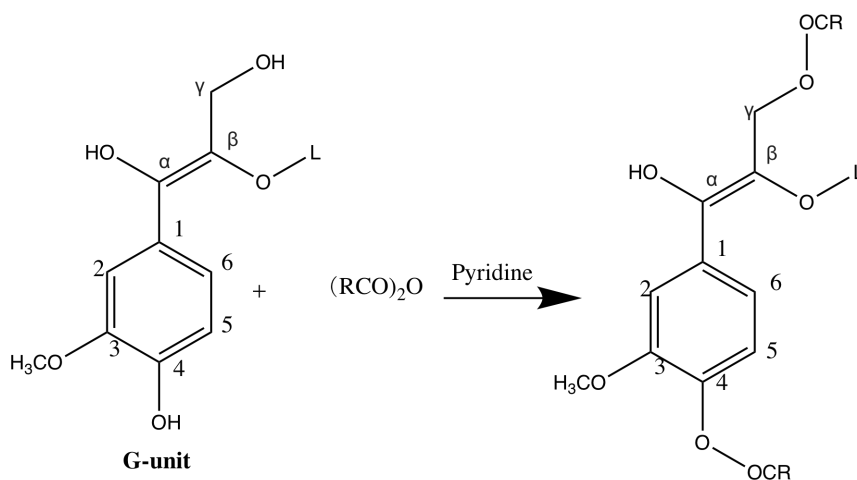
The appearance of the esterified lignin can be found in Figure 3.5. AcSKL has crystal-like powder texture with some reflection at the surface (Figure 3.5b) while PaSKL has bulk structure with lighter brown color compared with the other lignin samples (Figure 3.5c), similar to the LauSKL sample (Figure 3.5d). PaSKL and LauSKL showed great water barrier property during the washing step with water and methanol, which might be a proof of sound hydrophobic property when applying them on the coating ingredient with PLA. TFASKL shows darker color when comparing with the original SKL powder (Figure 3.5e).

³¹P NMR spectra

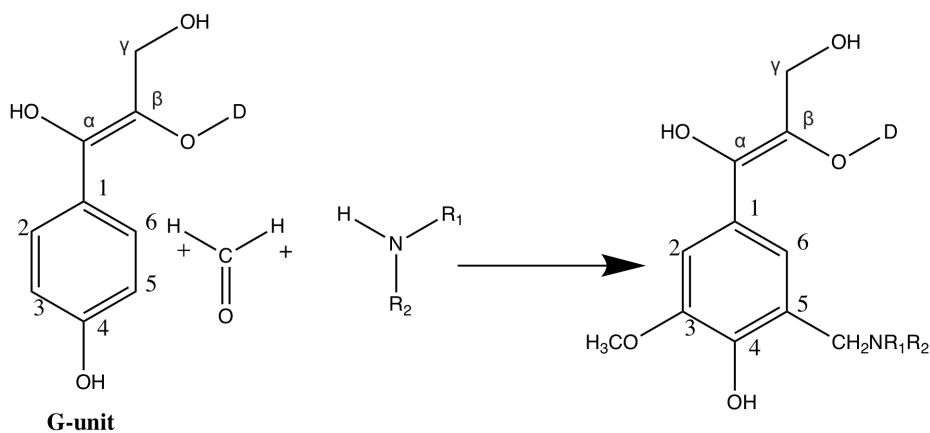
The obtained lignin samples were analyzed with different methods in order to see the modification extents.

Table 3.1: Amount of different hydroxyl groups in original SKL sample and the products after esterification, determined by ³¹P-NMR spectroscopy. The original data is obtained by duplicated determination. (Unit: mmol/g)

Name	Aliphatic OH	Condensed phenolic OH	G-OH	H-OH	Carboxylic OH
Original SKL	1.91±0.11	2.01±0.04	2.32±0.03	0.24±0.05	0.46±0.01
AcSKL	0.03	≈0.00	≈0.00	≈0.00	0.35
LauSKL	1.18	1.34	1.42	≈0.00	2.46
PaSKL	0.09	0.05	≈0.00	≈0.00	3.04
TrSKL	0.81	0.84	1.01	≈0.00	0.01



R=CH₃ Reagent: acetic anhydride, product denoted as AcSKL;
 R=CH₃(CH₂)₁₄ Reagent: palmitic anhydride, product denoted as PaSKL;
 R=CF₃ Reagent: trifluoroacetic anhydride, product denoted as TFASKL;
 R=CH₃(CH₂)₁₀ Reagent: lauric anhydride, product denoted as LauSKL;
 L= Connection with other parts of lignin structure.



R₁=R₂=CH₂CH₃ The Mannich reaction by diethylamine, product denoted as ManSKL;
 R₁=N(COO⁻)₂, R₂=COO⁻ The Mannich reaction by ED3A, product denoted as ED3ASKL.

Figure 3.4: The reaction of lignin modifications: esterification (top) and the two types of Mannich reactions (bottom).



(a) Freeze dried original SKL sample from LignoBoost process.



(b) Lignin derivative of acetic anhydride (freeze dried).



(c) Lignin derivative of palmitic anhydride (freeze dried).



(d) Lignin derivative of lauric anhydride (freeze dried).



(e) Lignin derivative of TFAA (freeze dried).

Figure 3.5: The lignin derivatives from esterification of different anhydrides. The appearance of the AcSKL is crystal-like and the PaSKL shows bulk structure with lighter color than the original lignin samples, so as the LauSKL, while the sample from the TFAA reaction has a darker color with crystal-like structure, too.

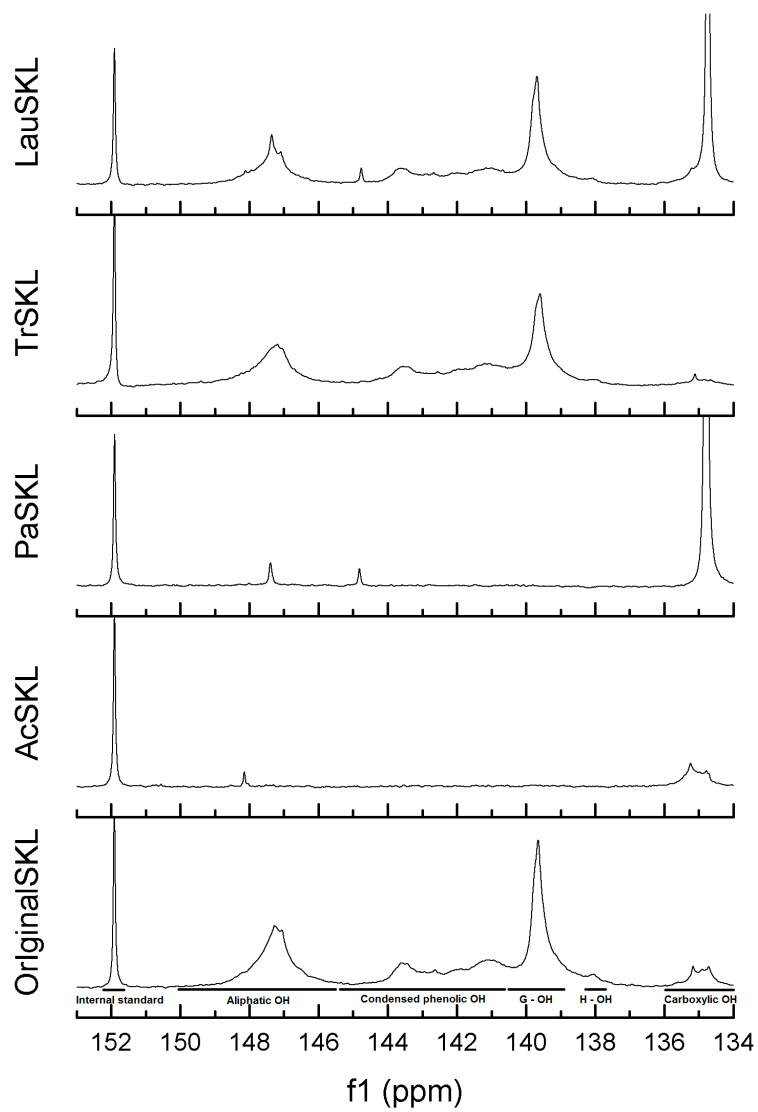


Figure 3.6: ^{31}P NMR spectra of SKL and different esterified SKL samples.

As shown from the ^{31}P -NMR analysis (Table 3.1 and Figure 3.6), the peaks of aliphatic and condensed phenolic hydroxyls almost disappear for AcSKL (only 0.03 mmol/g left of aliphatic OH) and PaSKL (0.09 mmol/g aliphatic OH and 0.05 mmol/g condensed phenolic OH) while decrease for the LauSKL (1.18 mmol/g aliphatic OH and 1.34 mmol/g condensed phenolic OH left) and TFASKL (around 0.81 mmol/g aliphatic OH and around 0.84 mmol/g condensed phenolic OH left). All the H-OH structures were esterified for the four modified samples. While the carboxyl hydroxyls were still intact for AcSKL and lower for the TFASKL, the ones in the PaSKL and LauSKL increased to higher amounts of 2.46 mmol/g and 3.04 mmol/g, respectively.

For the AcSKL sample, the esterification reactions were fully completed in the sample according to the analyzed results. Almost all the available hydroxyl groups were reacted in lignin. But the carboxyl hydroxyls content was kept still as in the original SKL, after washing off all the acetic acid formed during the decomposition process by water and evaporation. As for the PaSKL, the esterification reaction of all the aliphatic and phenolic hydroxyls were completed, too. However, it was based on conducting the experiment with one extra hour of reflux other than 24h of reaction at room temperature as in the AcSKL experiment. This may be related to the long aliphatic chain structure in the palmitic anhydride. The long aliphatic chain caused the steric hindrance and enhanced the difficulty of reaction. The use of long aliphatic anhydride also influenced the amount of carboxyl hydroxyl content in the lignin structure after the reaction. Theoretically, the original carboxylic groups in the PaSKL should remain constant as the one from AcSKL, in other words, similar to the original SKL. However, from the ^{31}P NMR result, almost 5 times of carboxylic OH was found in the PaSKL compared to the one from original SKL. Therefore, the increased amount of carboxylic groups should come from the free palmitic acid, which was generated from the decomposition of the palmitic anhydride left from the reaction. Since there is for now no effective way of purifying the PaSKL sample, the final product was a mixture of palmitic acid and lignin derivatives.

The same condition has been applied to prepare LauSKL. With the steric hindrance of long aliphatic chains in lauric acid, it is similarly difficult to proceed the reaction completely. In fact, other than one hour of reflux, the mole ratio of lauric anhydride and SKL was 1:1 instead of 4:1 like in PaSKL in this experiment because of the shortage of the lauric anhydride storage (1 g). Therefore, it is likely that the lack of enough amount of lauric anhydride resulted in the

uncompleted reaction as seen by ^{31}P -NMR analysis. However the amount of the final carboxylic hydroxyl content increased in the LauSKL (from 0.46 mmol/g to around 3.04 mmol/g), it is most likely that the LauSKL was also a mixture of free lauric acid formed from the unconsumed lauric anhydride and the lignin derivative. On the other hand, the left lauric acid could be a merit in the fertilizer coating application due to its hydrophobicity.

When it comes to the TFASKL, all the hydroxyl groups in the sample showed decreased trends as seen from the experimental results. However, not all the available hydroxyl groups were reacted. The reaction of esterification can not be proceeded completely. This might be attributed to the presence of huge fluorine atoms on the structure of trifluoroacetic anhydride (TFAA). Lignin, by itself, has a relatively compacted and irregular structure, so even though TFAA is a much stronger anhydride compared with acetic anhydride and palmitic anhydride, its extremely large steric hindrance still prevented it from reacting with all of the OH groups in lignin structure. On the other hand, the carboxylic hydroxyl content dropped down after the reaction between TFAA and lignin, which could be an evidence of acylation between TFAA and the lignin's carboxylic acid group which might form ester at the end.

FTIR spectra

All the samples were further analyzed for FTIR and the results can be found in enlarged Figure 3.7 and Figure 3.8.

Infrared spectra of the modified lignin samples have been compared with the spectrum of original SKL in order to reveal the extent of esterification reactions.

All the results were compared by using peaks at 1511 cm^{-1} as reference (the aromatic skeletal vibrations and ring breathing in lignin). The esterification reactions of AcSKL, PaSKL, and LauSKL resulted in decreases in the hydroxyl groups in lignin samples, according to the descending and shifting peaks around 3377 cm^{-1} (the stretching of hydroxyl groups in phenolic and aliphatic structures). On the contrary, TFASKL sample showed mainly the same trend as the original sample around this wavenumber; corresponding to the similar amount of phenolic hydroxyl groups analyzed above; in an agreement with observations in NMR experiments. A trend of increasing area with signal maximum at 2935 cm^{-1} and 2840 cm^{-1} (C-H stretch in aliphatic $-\text{CH}_3$ and $-\text{CH}_2-$ groups, asymmetric and symmetric respectively) were observed for PaSKL and

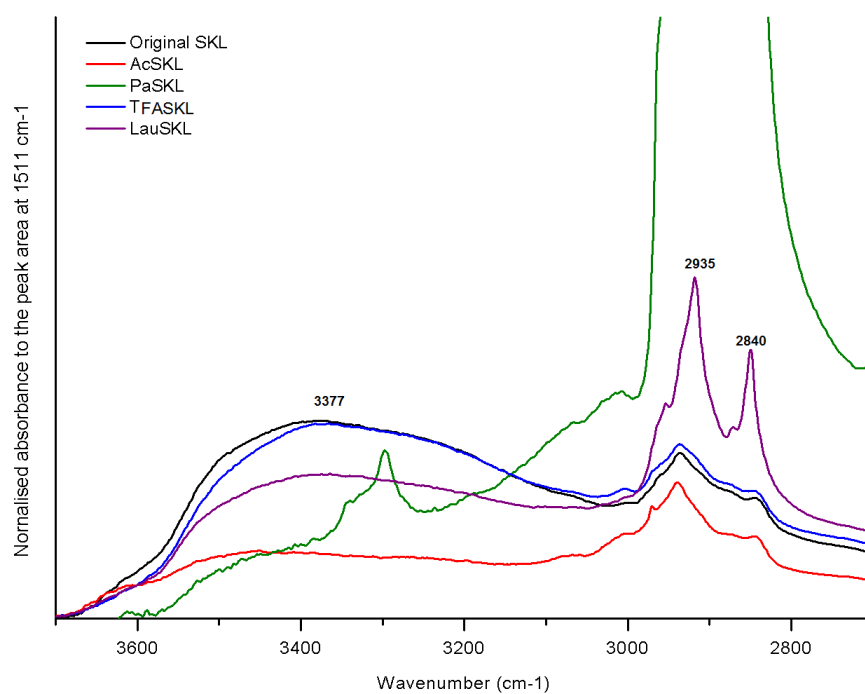


Figure 3.7: FTIR spectra of original SKL sample and the esterified samples. Wavenumber between 3700 to 2700 cm⁻¹.

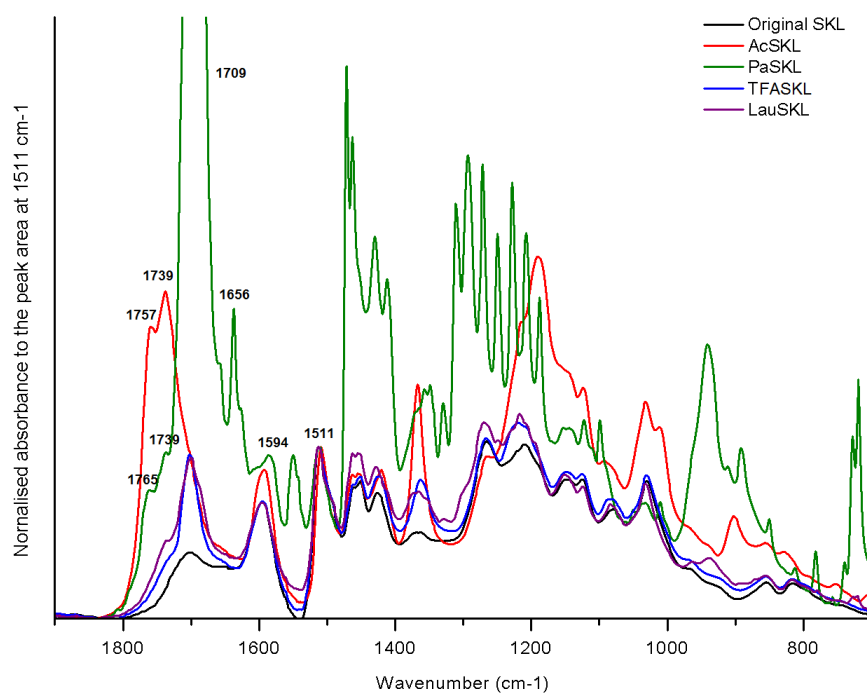


Figure 3.8: FTIR spectra of original SKL sample and the esterified samples. Wavenumber between 1900 to 700 cm^{-1} .

LauSKL samples. This may correspond to the addition of long aliphatic chains in the lignin structure, as well as the remaining carboxylic acids. Furthermore, for samples AcSKL and PaSKL, increased peaks at 1757 cm^{-1} (1765 cm^{-1} for PaSKL) and 1739 cm^{-1} were observed. These were attributed to the esterified form of aromatic and aliphatic alkanoxy groups, respectively. The broadening peaks around 1708 cm^{-1} for sample PaSKL, LauSKL and TFASKL were assigned to carbonyl stretching of ester and carboxyl groups in lignin, i.e. the existence of C=O. This may be attributed to the remaining carboxylic acids.

These results indicated that the formation and the presence of the carboxylic OH groups was resulted from the replacing hydroxyl groups with acylated groups in lignin structure. In other words, it gave evidence of the esterification reactions in AcSKL, PaSKL and LauSKL.

TFASKL was not esterified extensively as expected according to the FTIR spectrum. Instead, the hydroxyl groups remained the same as the ones in the original SKL sample.

Two-dimensional ^1H - ^{13}C NMR spectra (2D NMR)

Two-dimensional ^1H - ^{13}C NMR spectra (2D NMR) were conducted on all the samples in order to provide structural information of samples in two frequency dimensions (^1H - ^{13}C). Data of esterified samples were compared with the original SKL. According to the mechanism of esterification reactions, the reactions provided new functional group connections close to C_α , C_γ and C_4 position. This may lead to the signal shifts of neighbouring $\text{C}_\beta\text{-H}_\beta$ and $\text{C}_5\text{-H}_5$ peaks to new signal regions. As seen in Figure 3.9 and 3.10, both AcSKL sample and PaSKL have a shifted $\text{C}_5\text{-H}_5$ peak at $\delta_{\text{C}}(\text{ppm})/\delta_{\text{H}}(\text{ppm})$ 122.18/6.96 and $\delta_{\text{C}}(\text{ppm})/\delta_{\text{H}}(\text{ppm})$ 127.51/7.10, respectively. Peaks of $\text{C}_\gamma\text{-H}_\gamma$ also show different values in the side chain regions ($\delta_{\text{C}}(\text{ppm})/\delta_{\text{H}}(\text{ppm})$ at 63.07/3.98 and 60.87/3.97, respectively). These results verified the esterification reactions on the AcSKL and PaSKL samples at C_α , C_γ and C_4 position. However, peaks of $\text{C}_5\text{-H}_5$ and $\text{C}_\gamma\text{-H}_\gamma$ remain the same in the figure of TFASKL. The lignin sample was therefore not extensively esterified, which agreed to the FTIR and NMR analyzing results. Furthermore, peaks of $\text{C}_5\text{-H}_5$ and $\text{C}_\gamma\text{-H}_\gamma$ in the LauSKL sample also remain the same as the original one. It is, however, not in an agreement with results in the NMR and FTIR spectra, both of which indicated the esterification reaction in the LauSKL. It can be explained by the incomplete reaction due to the lack of lauric anhydrid reagent at the beginning. Only a small part of the hydroxyl groups were replaced in the reaction,

while most of the hydroxyl groups in the G-units still remained. The final shifted signals of C₅-H₅ and C_γ-H_γ linkages were therefore too small to be detected in this study.

The TFASKL sample was not used in the following study since it was not esterified successfully.

3.1.3 Amination of lignin: the Mannich reactions

The Mannich reaction by diethylamine

G-unit, the almost sole aromatic ring type in the SKL lignin structure which contains free C-5 positions on the aromatic ring, was considered to be reactive for amination. As seen in Figure 3.4, G-unit in the SKL sample is considered to react with diethylamine and formaldehyde and form structure with short ethylamine side chain. Figure 3.11 demonstrates the appearance of the SKL sample after the Mannich reaction. The sample showed a fluffy structure with light brown color. Table 3.2 and Figure 3.12 demonstrates the amount of different hydroxyl groups determined by ³¹P-NMR spectroscopy. As shown, the peak of phenolic G-OH (139.0-140.2 ppm) disappears from the curve after the reaction. It gave an evidence of the completion of the Mannich reaction. C5 site on the G-unit was attacked by the dialkylaminomethyl, led to a peak appeared at the range of 145.4-143.0 ppm. Meanwhile, all the other hydroxyl groups remained the same as in the original SKL sample. This is to some extents, good when ManSKL is used as a coating layer component of fertilizers, because the remained phenolic groups in SKL structure were suggested to be involved in the process of preventing urea from hydrolysis and microorganism nitrification.

FTIR spectrum (Figure 3.13) of the ManSKL shows stronger peak of the hydroxyl groups in the lignin sample, by the increasing peak around 3377 cm⁻¹ (the stretching of hydroxyl groups in phenolic and aliphatic structures). In addition, a new strong signal of -N(CH₂CH₃)₂ can be found at around 2950 cm⁻¹ on the ManSKL curve, when comparing it with the curve of original SKL sample. These further confirmed the introduction of new dialkylaminomethyl groups.

2D NMR (Figure 3.14) also shows a new peak at $\delta_C(ppm)/\delta_H(ppm)$: 58.66/3.58, corresponded to the signal of -N(CH₂CH₃)₂. Furthermore, the disappearance of C₅-H₅ signal further verified the complete substitution at almost all C₅ positions.

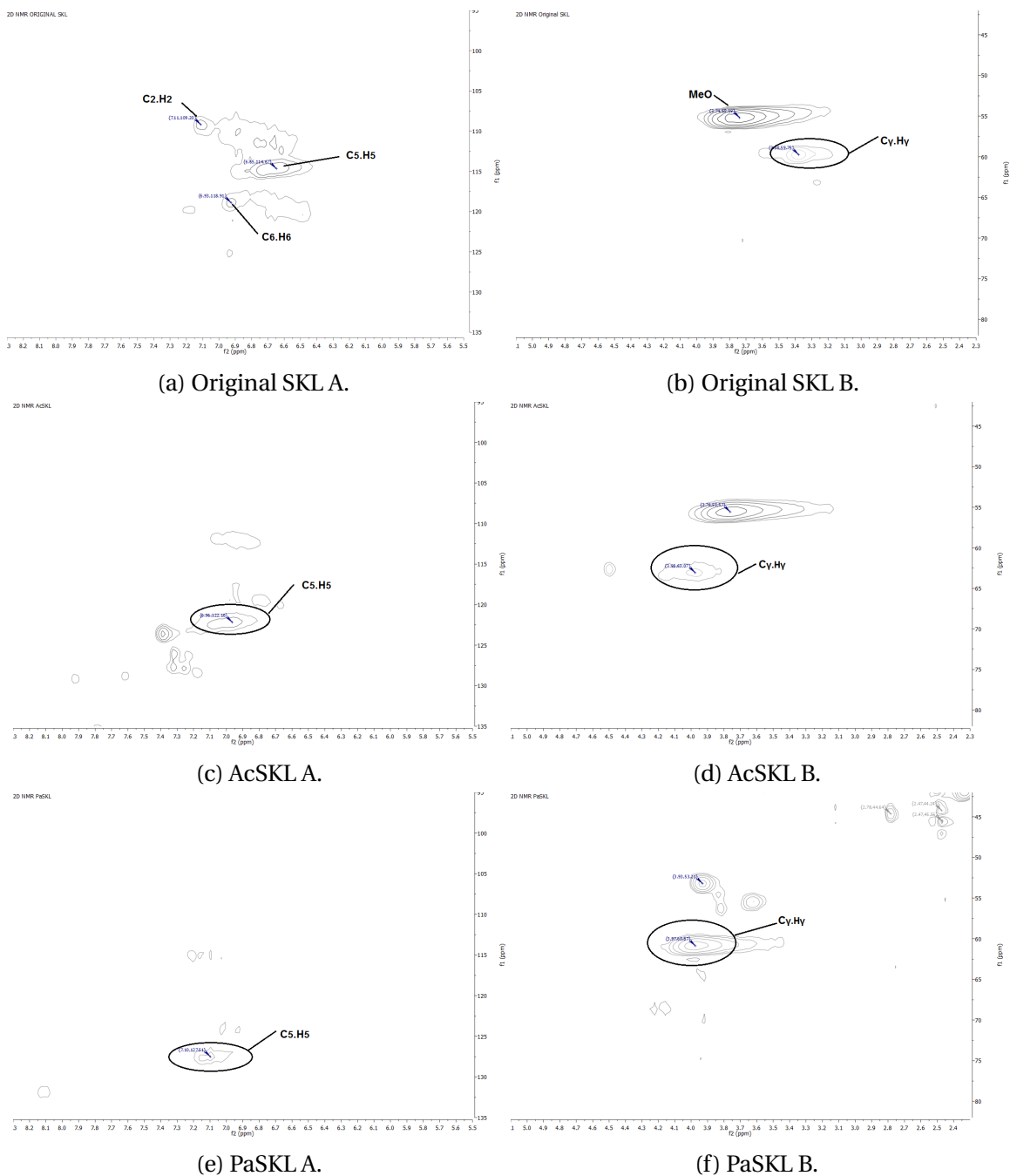


Figure 3.9: Aromatic regions (A: $\delta_C(ppm)/\delta_H(ppm)$ 43-82/ 2.3-5.1) and Side-chain regions (B: $\delta_C(ppm)/\delta_H(ppm)$ 97-135/ 5.5-8.3) in the 2D HSQC NMR spectra of original SKL and esterified lignin samples.

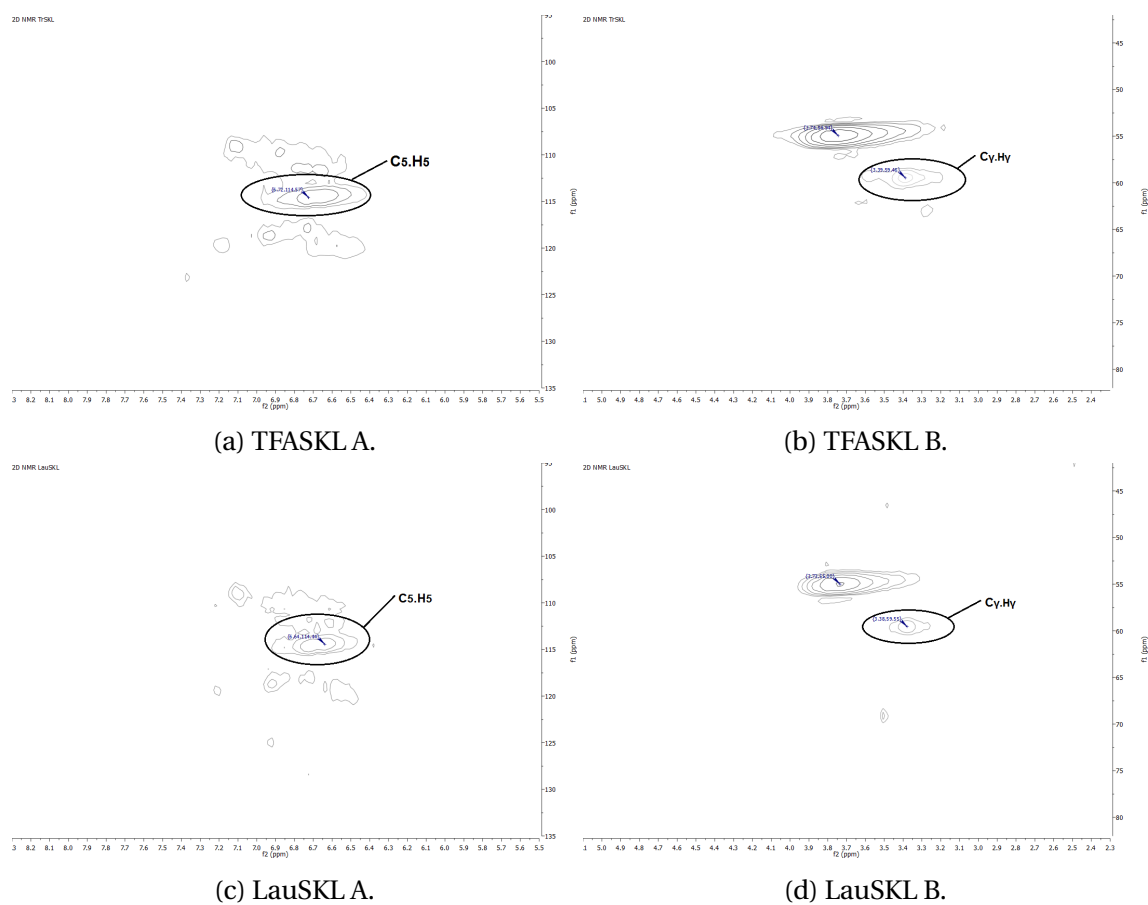


Figure 3.10: Aromatic regions (A: $\delta_C(ppm)/\delta_H(ppm)$ 43-82/ 2.3-5.1) and Side-chain regions (B: $\delta_C(ppm)/\delta_H(ppm)$ 97-135/ 5.5-8.3) in the 2D HSQC NMR spectra of original SKL and esterified lignin samples.



Figure 3.11: The ManSKL sample after freeze drying, with light brown color and fluffy structure.

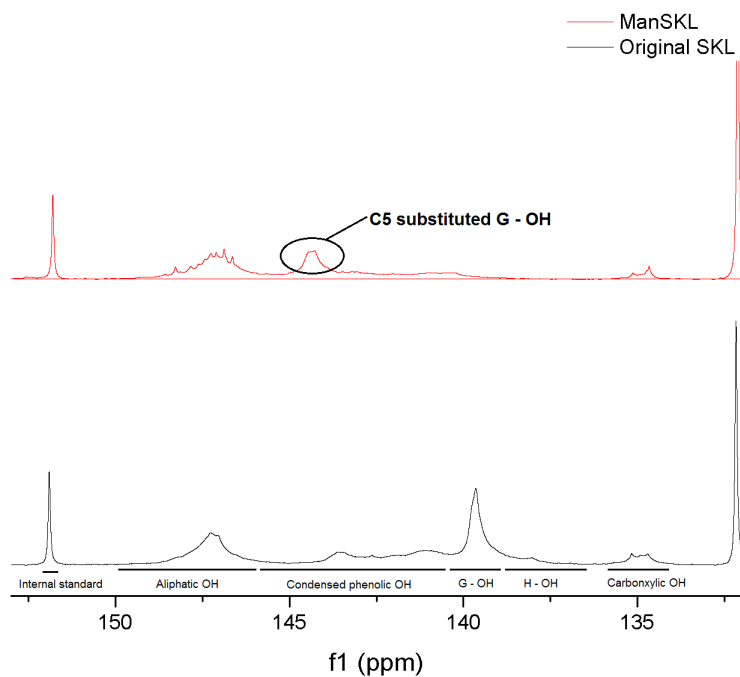


Figure 3.12: ^{31}P NMR spectra of original SKL sample and the product after the Mannich reaction by diethylamine.

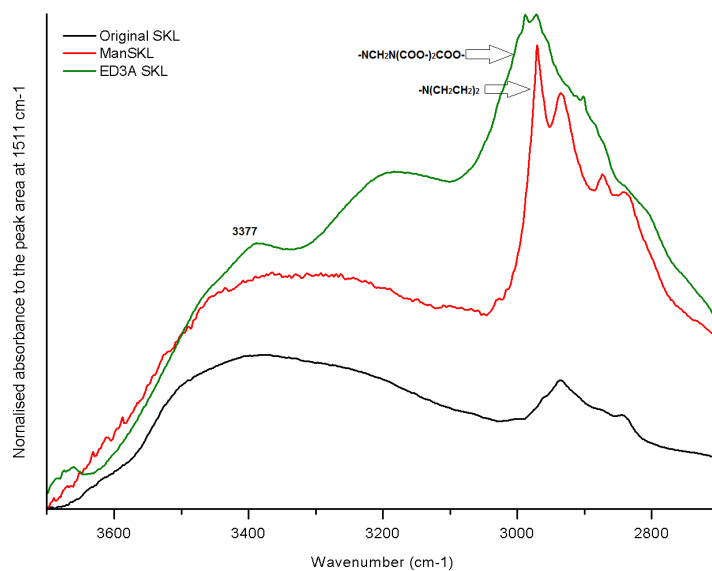


Figure 3.13: FTIR spectra of original SKL sample and the products after the Mannich reaction by diethylamine and ED3A. New peaks at around 2950 ppm^{-1} shown up on the curves of ManSKL and ED3ASKL

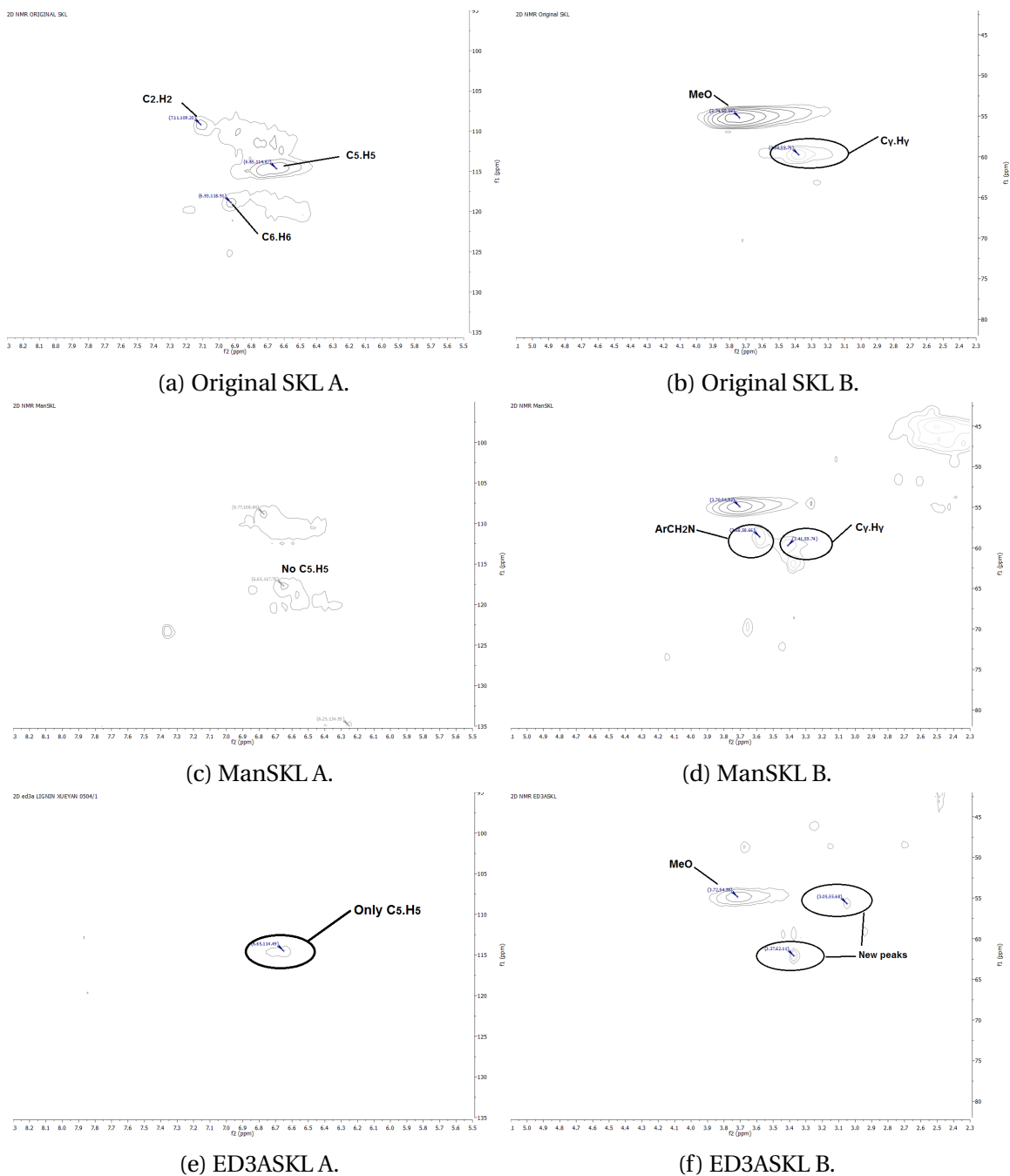


Figure 3.14: Aromatic regions (left column; δ_C/δ_H 43-82/ 2.3-5.1) and Side-chain regions (right column; δ_C/δ_H 97-135/ 5.5-8.3) in the 2D HSQC NMR spectra of original SKL and SKL sample after the Mannich reactions.

Table 3.2: Amount of different hydroxyl groups in original SKL sample and the product after the Mannich reaction by diethylamine, determined by ^{31}P -NMR spectroscopy. The original data is obtained by duplicated determination (Unit: mmol/g)

Name	Aliphatic OH	Condensed phenolic OH	G-OH	H-OH	Carboxylic OH
OriginalSKL	1.91±0.11	2.01±0.04	2.32±0.03	0.24±0.05	0.46±0.01
ManSKL	1.70	≈1.31	≈0.00	≈0.00	0.21

The Mannich reaction by ethylenediaminetriacetic acid (ED3A)

ED3A is another amine that was used in this study to conduct the Mannich reaction.

ED3A qualitative analysis Before using ED3A for the Mannich reaction, it needs to be analyzed to see whether the solution prepared following the method mentioned above contains ED3A or not. In order to give a proof of existence of ED3A in the final prepared solution, NMR analysis was conducted.

The C- and H-NMR spectra of synthesized ED3A solution are displayed in Figure B.2 and Figure B.1, respectively (Appendix B). The peaks of H atoms and C atoms from the synthesized ED3A solution agree with the data from Qiongxin Liu (2010); the corresponding data can be found in Table 3.3, and Table 3.4. These results revealed the structure of ED3A (Figure 1.9), therefor fully proved the existence of ED3A in the solution.

Table 3.3: Assigned ^{13}C NMR spectra data of ED3A

Compound	α -CO ₂	β -CO ₂	β' -CO ₂	α -CH ₂ CO ₂	β -CH ₂ CO ₂	β' -CH ₂ CO ₂	-CH ₂ N	-CH ₂ N'
ED3A	172.41	170.40	168.17	57.44	54.46	51.90	48.22	46.06

Table 3.4: Assigned ^1H NMR spectra data of ED3A

Compound	s, CH ₂	t, J-CH ₂	s, CH ₂	s, CH ₂	t, J'-CH ₂
ED3A	3.94	3.46	3.28	3.12	3.06

Amination of lignin model compound by ED3A To have a better understanding of the Mannich reaction of ED3A on the softwood kraft lignin structure, a lignin model compound, vanillyl alcohol was selected in this study due to its structural similarity as the G-unit in lignin (Fig. 2.1). The ^{13}C NMR analysis was used to give a overall look of the reaction.

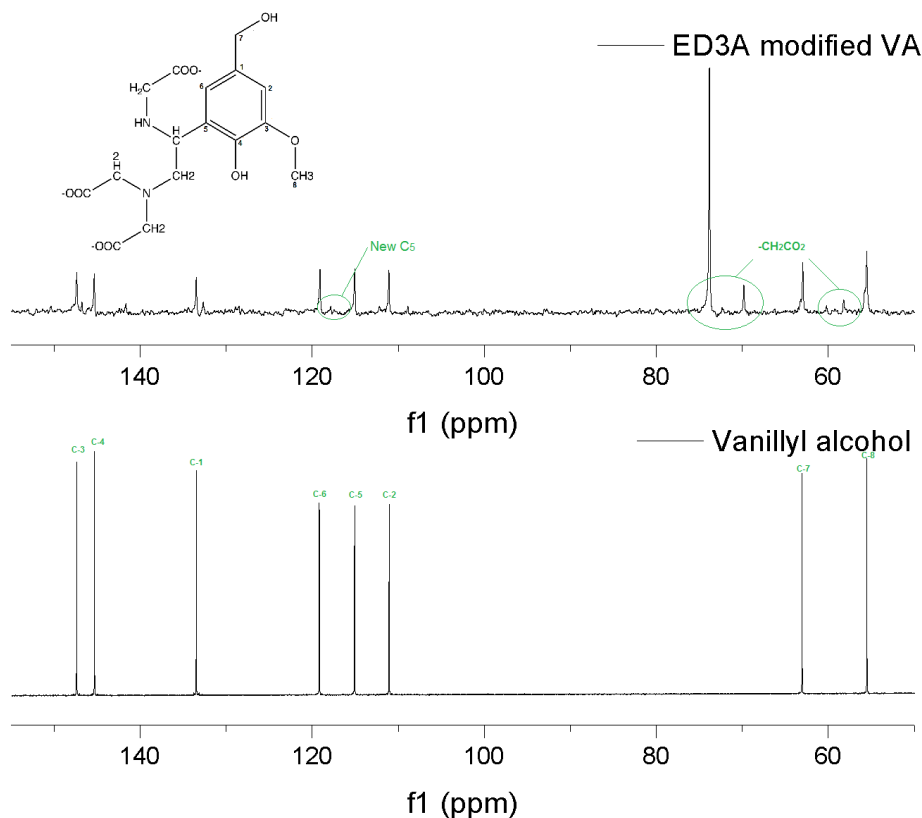


Figure 3.15: ^{13}C NMR spectra of vanillyl alcohol and ED3A modified vanillyl alcohol sample.

As seen in Figure 3.15, in addition to the original C-5 signal (114.71 ppm), there is a new peak shifted from the original one to 117.32 ppm due to the partially introduction of amine group onto the C-5 position of the aromatic ring. Besides, three new peaks have been observed and identified (73.60 ppm, 69.61 ppm, 57.75 ppm), which are the new $-\text{CH}_2\text{CO}_2$ signals on the ED3A structure after the Mannich reaction.

2D-NMR analysis was also conducted to monitor this reaction. As shown in Figure 3.16, the original aromatic $\text{C}_5\text{-H}_5$ signal still remains. However, since there is a limitation of 2D NMR that it cannot provide an accurate quantitative data, it is difficult to determine whether the vanillyl alcohol has been partly modified. On the other hand, at the regions around $\delta_{\text{C}}(\text{ppm})/\delta_{\text{H}}(\text{ppm})$: 57.49/4.45, 69.10/3.50, and 73.02/4.54, shifts of $-\text{CH}_2\text{CO}_2$ have been observed (Figure 3.17). These peaks verified the introduction of ED3A amine groups onto the model compound.

Amination of softwood kraft pulp lignin by ED3A Experimentally, all the reaction parameters applied on the model study were used again on the SKL sample and the same structural analyses

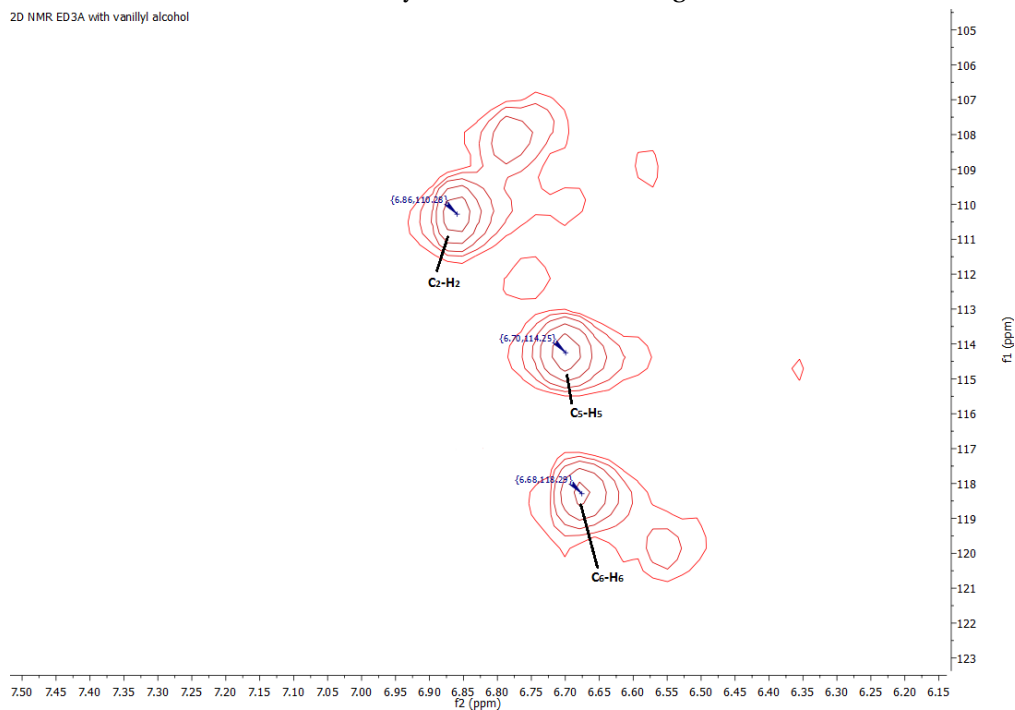
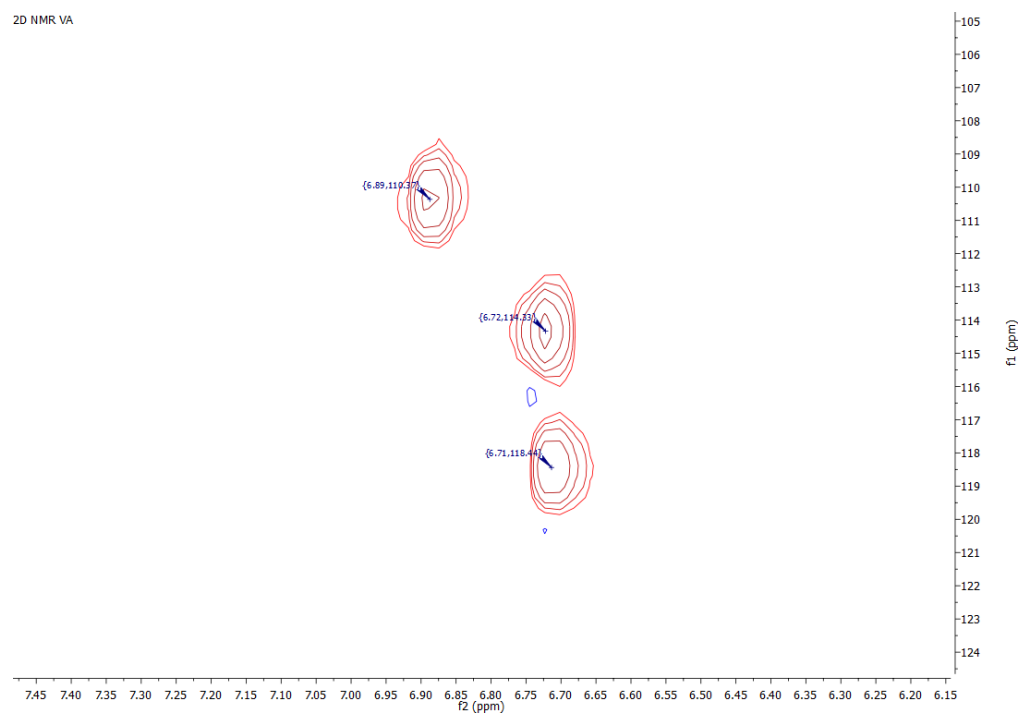
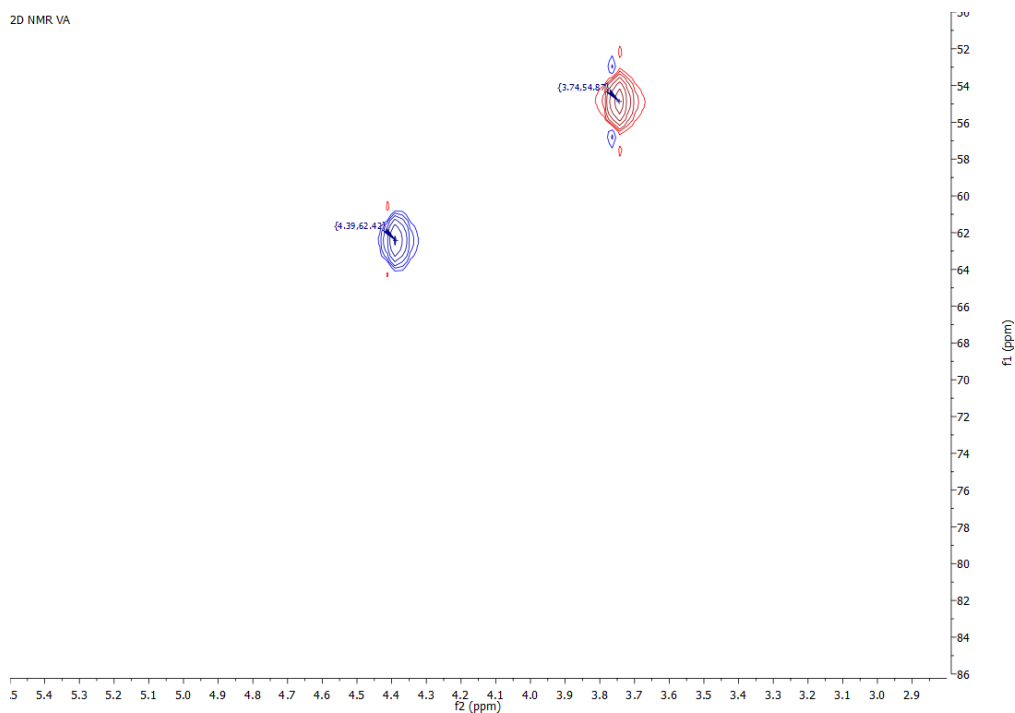
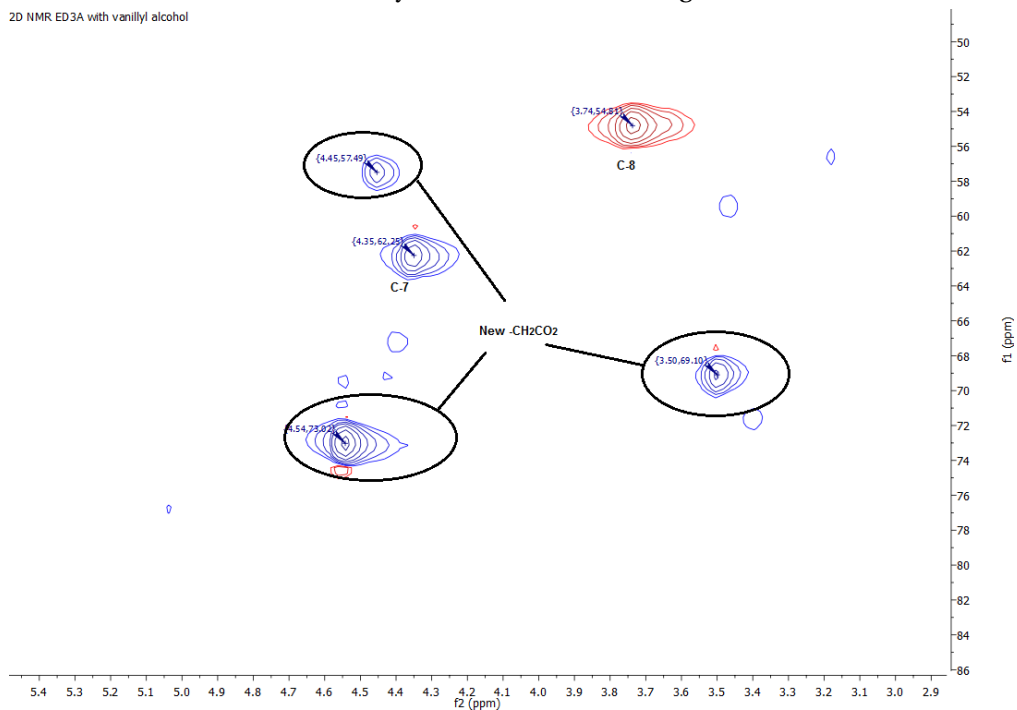


Figure 3.16: 2D HSQC NMR spectra at aromatic C-H region of model compound: vanillyl alcohol, and synthesized ED3A modified model compound.



(a) Vanillyl alcohol (side chain region).



(b) ED3A modified model compound (side chain region).

Figure 3.17: 2D HSQC NMR spectra at side chain C-H region of model compound: vanillyl alcohol, and synthesized ED3A modified model compound.

were proceeded, too.

^{13}C NMR analysis was conducted first on the ED3ASKL sample. However, no signal was detected due to the low solubility of ED3ASKL. Many other solvents were tried but the ^{13}C NMR analysis showed the same result because of the low solubility. Therefore, other analyses were conducted instead.

As for FTIR analysis, a new peak of ED3A groups at around 2980 ppm^{-1} appears in the ED3ASKL spectrum as can be seen in Figure 3.13. This may be an evidence of introducing of new ED3A groups on the lignin structure.

Figure 3.14 shows the 2D NMR spectra of ED3ASKL sample. In the figure, only the peak of $\text{C}_5\text{-H}_5$ appears in the aromatic region. There is no peak of $\text{C}_2\text{-H}_2$ and $\text{C}_6\text{-H}_6$. Moreover, the peak of $\text{C}_\gamma\text{-H}_\gamma$ disappears in the side chain region. Instead, two new peaks can be observed at $\delta_{\text{C}}(\text{ppm})/\delta_{\text{H}}(\text{ppm})$: $55.68/3.05$ and $62.11/3.37$. The disappearance of these main C-H linkages in the G-units were not in an agreement with the Mannich reaction of ED2ASKL. The reaction mechanism between ED3A and lignin was therefore not following the Mannich reaction as shown in the Figure 3.4. ED3A did not react at C_5 position in the lignin sample, at least not as the main reaction. The possible reason might be the high steric hindrance between ED3A and lignin structure. Obviously for this lignin modification by ED3A, the mechanism of the reaction still need to be investigated.

Since the ED3ASKL was not modified successfully as expect in this study, it was not used in the following experiment. However, successful reaction between ED3A and vanillyl alcohol has already demonstrated a good approach for the future investigations of ED3ASKL.

3.2 Coating urea pellets

There are many coating methods available nowadays when it comes to fertilizer coating. However, as mentioned in the introduction part, most of the coating procedures require expensive mechanical instruments and complicated systems setting. It is valuable to simplify the preparation technique of slow release fertilizer in order to lower the production costs.

The coating approach of dip-coating technique has been applied by some researchers as cheaper and simpler proceeding process in solution state; the coating material is dissolved in a

solvent, followed by immersing an inner material into the solution and taking it out for drying afterwards. It is an attractive technique which has been used here in this study.

3.2.1 Solvent selection

The principle of the dip coating technique is that the inner material should have relatively low solubility in the solvent. In this study, urea is used as the core fertilizer and it is a well known water soluble chemical, in addition, it can be dissolved in other polar solutions. Therefore, the solvent used in this case needs to be nonpolar or polar aprotic. Moreover, considering the components chosen for coating here were lignin and PLA, several solvents for both of them were considered as candidates.

PLA dissolution has been investigated by [Sato et al. \(2013\)](#), where the Hansen solubility parameter (HSP) was used as one judgment to determine dissolution effect of organic solvents for PLA. Three parameters, hydrogen bonding solubility parameter (δ_h), polar solubility parameter (δ_p) and dispersion solubility parameter (δ_d) were plotted as a point in a three dimension structure on three mutually perpendicular axes as to quantify the solubility degree of different solvents. And after comparing these parameters with the dissolving results from actual experiments, the conclusion was that hydrogen bonding parameter is the most important one in the solubility, and PLA was soluble in polar aprotic solvents but insoluble in polar protic or nonpolar solvents.

Table 3.5: Hansen solubility parameter of DCM and chloroform. Data obtained from [Sato et al. \(2013\)](#). The total HSP (δ_t) is obtained from the equation: $\delta_t^2 = \delta_p^5 + \delta_d^2 + \delta_h^2$. (Unit: $\text{MPa}^{1/2}$).

solvent	Solvent type	δ_d	δ_p	δ_h	δ_t	Result
Dichloromethane (DCM)	Polar aprotic	18	12.3	7.2	22.9	soluble
Chloroform	Polar aprotic	17.8	3.1	5.7	19	soluble

Dichloromethane (DCM) and chloroform were two solvents which are most commonly used as dissolving agents of PLA. Both of them are polar aprotic solvents, but DCM is less toxic. Furthermore, DCM has a higher calculated value of HSP parameter (as seen in Table 3.5), so it was chosen in this study.

However, SKL and all its derivatives made in this study are insoluble in DCM solvent, thus another solvent needs to be added to make sure a good mixing of PLA and the lignin. Ace-

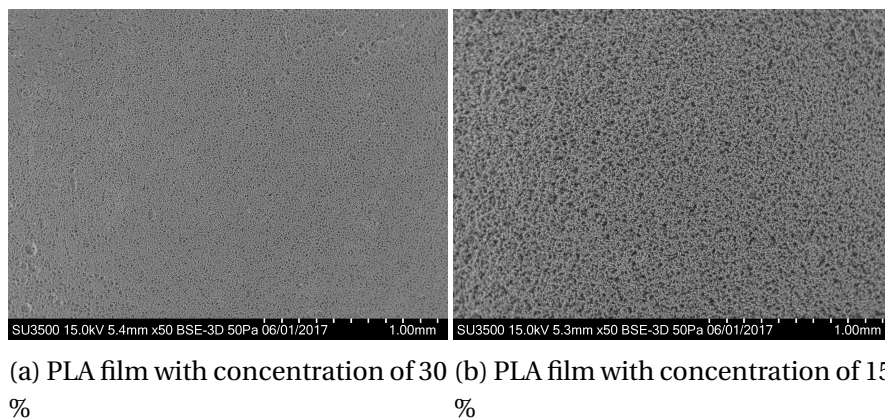


Figure 3.18: SEM images (magnification times: $\times 50$) of cast films from PLA with different concentrations. Left: 30 %, right: 15 %.

tone, dioxane and tetrahydrofuran (THF) were well-known for their sound abilities of dissolving lignin. Acetone was first used in the experiment to mix lignin with the PLA solution. But after conducting the experiment, the result showed that lignin was precipitated instead of well-dissolved in the mixed solution. Although the miscibility between acetone and DCM was good, lignin could not even be dispersed well in the solution. Therefore, acetone was not used anymore in the later experiments. Furthermore, THF is less toxic compared to dioxane although both show similar lignin dissolution capabilities. With a sound miscibility with DCM, THF was thus used as the solvent for lignin and its derivatives. The mix solution of DCM and THF became the dip coating solution in this study at the end.

3.2.2 Film casting and its evaluations

Due to the similarity between formation of dip coating layer and film casting from solution, film casting was conducted to evaluate the final coating quality. Teflon Petri-dishes were used here because of the sticky character of the solution.

Concentration dependence

There are several factors that contributed to the quality of final films. For film formation, the coating material by itself should have a stable forming behavior with a sound and stable mechanical properties. It should not be brittle but with a fine elasticity, so that the structure of the film could be uniform and without pores, and the forming coating layer does not peel off or

break.

It has been found that the concentration of PLA in the film casting solution plays an important role when casting the film, mainly because PLA is inherently brittle. When the concentration of PLA in the solution is too high, the final PLA film formed will be too thick to maintain enough elasticity and thus will be easy to break. However, if the PLA/DCM solution concentration is too low, pores and imperfect structure may form on the film. This may lead to urea dissolution when used in urea fertilizer coating system.

In this study, three concentrations (15 %, 30 % and 60 %) of PLA solutions were prepared. They were then mixed with the original lignin sample/THF (6 %, w/v) solution at volume ratio of 1:1. After film casting on the petri-dish, all the films were inspected and analyzed by SEM determination.

Results show that the film formed from the concentration of 60 % featured the worst elasticity, with observable clear cracks on the film. Samples from concentration of 15 % and 30 % have similar performances, but the one from 30 % PLA has a smoother and flatter surface. SEM analysis was conducted on both films, and the results can be seen in Figure 3.18, which shows that the one from 30 % PLA is a uniform film, with less pores on the film surface. Considering the subsequent operation of multiple coatings, the concentration of PLA of 30 % would lead to a better effect, e.g. without the problem of old PLA layer re-dissolution in the new coming solution used for the repeated coating. Therefore, PLA/DCM solution with 30 % concentration was selected in this study to conduct further investigations and coating repetitions.

Ratio between DCM and THF

Evaporation rate difference of different solvents in the mixed solution is also an important factor here which would influence the outcome of the dip coating results. DCM has boiling point of 39.6 °C, whereas THF has 66 °C. Different boiling points lead to different evaporating rates and uneven evaporation will change the mixed solution concentrations of different solvents, causing precipitation of the coating components. This will influence the final film quality. In this study, different ratios of DCM and THF (v/v: 5:0, 4:1, 3:2, 2:3, 1:4, and 0:5) have been changed to make the mixed solution (using AcSKL in lignin concentration of 6 %) in order to reveal the influence of evaporation behaviour from all these film casting solutions. Identically these lignin solutions

were prepared by mixing PLA/DCM solution (30 %, w/v) with the lignin solution and poured onto Petri-dishes followed by air-drying.

Films appearance As seen in Figure 3.19, different dried films form from different ratios of DCM and THF in the solutions. Sample 1) from 100 % DCM as solvent showed the best performance, uniform film without visible cracks at the surface. However, the distribution of lignin was uneven (The film showed darker color compared with other samples) due to the lack of THF so that the mixed solution has the lowest lignin solubility. With the increasing amount of THF in the solution, lignin became more dispersed in the formed films, which explained the lighter colors in samples 3), 4), 5) and 6). On the other hand, the ascending amount of THF results in the evaporation status changed. DCM evaporated first from the film so that THF concentration increased. Since PLA has a poor solubility in THF, big cracks showed up on the films of samples 5) and 6). Overall, sample 3) and sample 4) showed the best film performance among all films due to balances between the DCM and THF effects. But it is worth mentioning that even though big cracks existed on samples 5) and 6), when it is applied for urea coating layer, the cracks were not formed since the superficial area of urea is much smaller than the Petri-dishes (see SEM analysis section).

Contact angle Since the coating layer of fertilizer is acting as a physical barrier to protect urea pallet from water, it is valuable to analyze the hydrophobicity of the coating layer. The film's hydrophobicity data could supply useful information to reveal the water barrier capability of final coating layers. Therefore, contact angle determinations were conducted on the films in order to understand the influence on the structure of different films from solution evaporation which is in turn related to the THF/DCM ratio in the solution. As seen from Figure 3.20 and Table 3.6, with the addition of THF in the PLA/SKL film solution, the contact angle of the films increase from 62.81° to 117.79°, following by a decreasing trend till 96.88°. The wettability of the film came to the lowest when the DCM/THF is 3:2. According to Wenzel (1936), the film wettability is related to the micro and nanoscale roughness of the surface and the evaporating process of THF/DCM may thus have an impact on the surface roughness of the films.

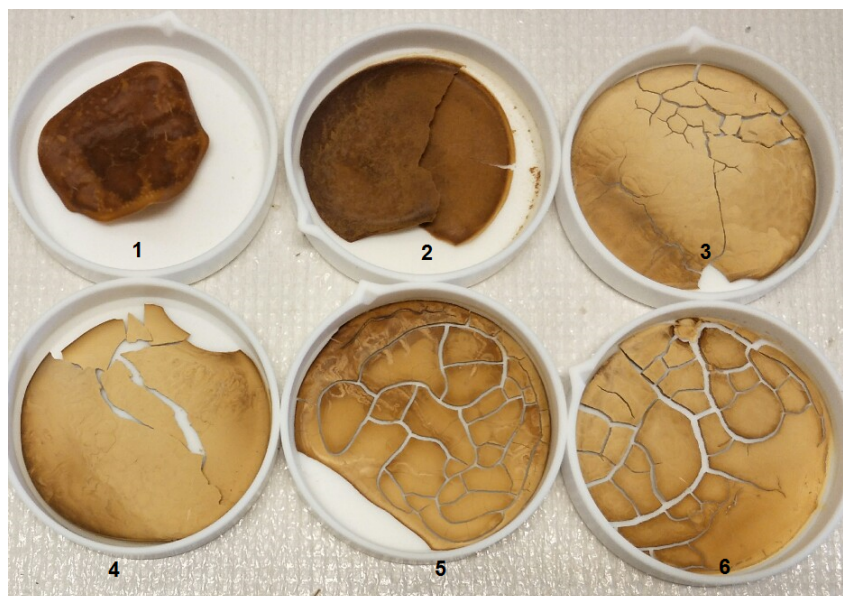


Figure 3.19: Casted films of PLA and AcSKL samples with different solvents composition. DCM/THF (v/v) = 1). 5:0; 2). 4:1; 3). 3:2; 4). 2:3; 5). 1:4; 6). 0:5.

SEM analysis SEM data further verified the above mentioned hypothesis (Figure 3.21 and Figure 3.22). PLA formed different semi-crystal structures during evaporation. With higher DCM ratio, samples 1) and 2) formed films with large PLA conjunctions sized around 30 to 60 μm . This may be related to higher evaporating rates of these solvents. PLA formed irregular shapes with few gaps in between. In samples 3), 4), 5) and 6), the films have relatively flat surface (Figure 3.21e, 3.21g, 3.22a and 3.22c) with micro-holes, sized around 10 to 20 μm , and small PLA fibre entanglements. The lower evaporating rates due to the increasing amount of THF in these samples affected the PLA semi-crystal shape. Furthermore, small size of imperfections lead to low toughness, as well as low wettability. Sample 3), therefore, has the lowest roughness with a more even fibre oriented surface and the highest hydrophobicity among all the tested samples.

Table 3.6: Contact angle (θ) values of PLA/AcSKL films, with different ratio of DCM and THF (Unit: $^\circ$) (SD: Standard deviation).

DCM/THF	5:0	4:1	3:2	2:3	1:4	0:5
Mean value	62.81	100.80	117.79	110.64	97.45	96.88
SD	1.89	1.92	2.36	5.04	6.03	2.33

According to the above results, the ratio of DCM/THF in sample 3) (3:2) was selected in the later coating process due to its better performance.

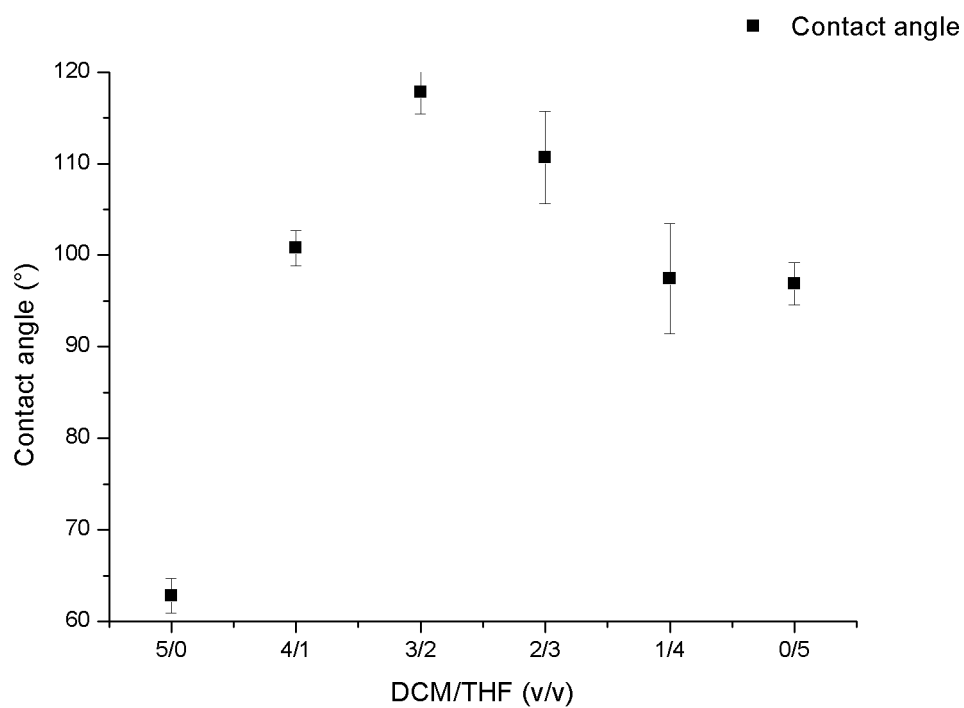


Figure 3.20: Contact angles of PLA/AcSKL blend samples using different solvent ratios. DCM/THF (v/v) = 1). 5:0; 2). 4:1; 3). 3:2; 4). 2:3; 5). 1:4; 6). 0:5.

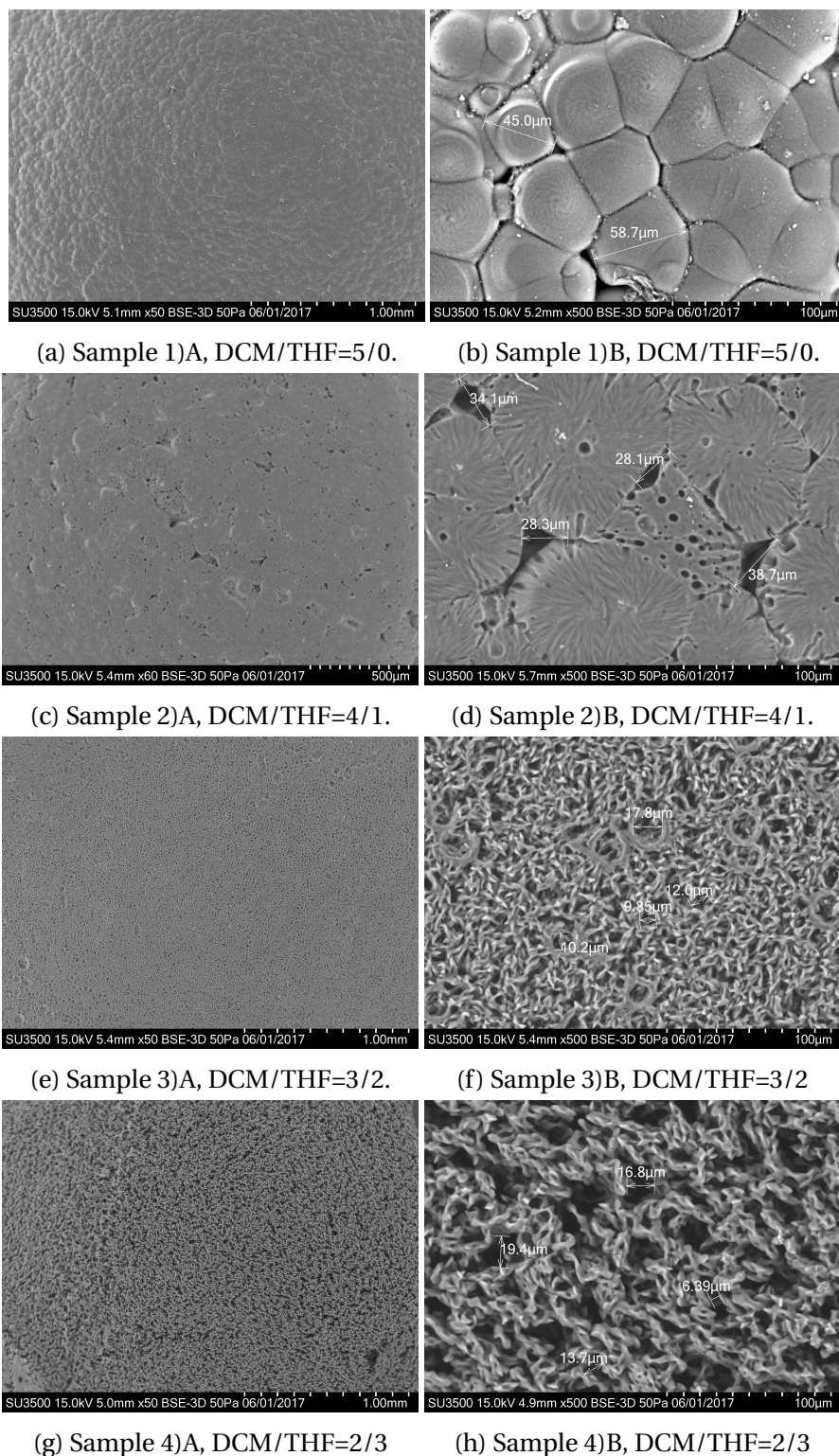


Figure 3.21: SEM images (magnification times: left column: $\times 50$; right column: $\times 500$.) of cast films from PLA solution with different ratio of DCM/THF (v/v) = 1). 5:0; 2). 4:1; 3). 3:2; 4). 2:3.

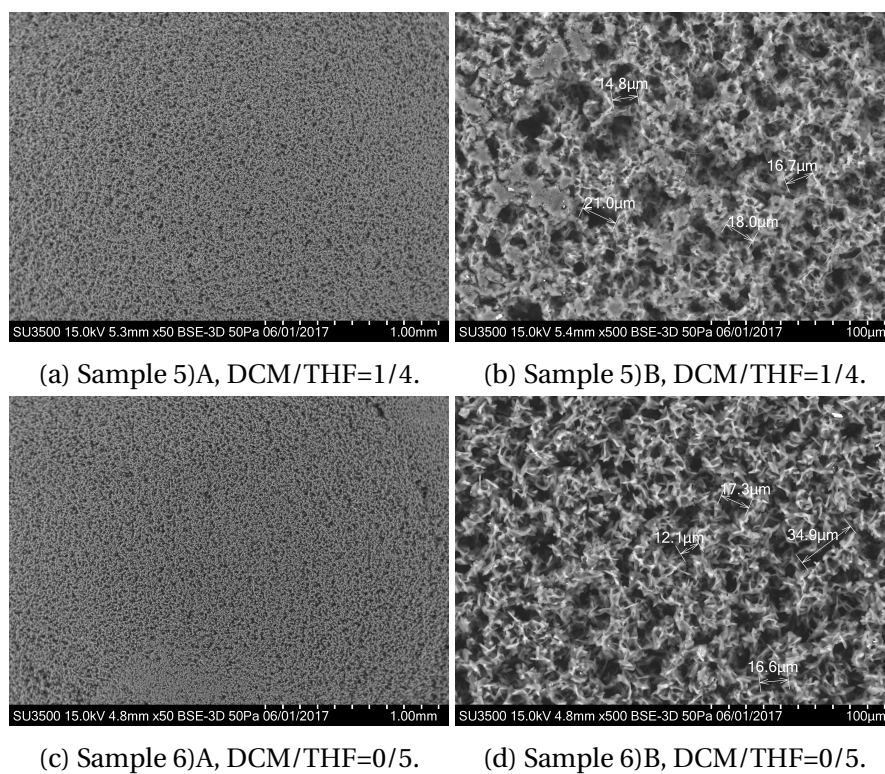


Figure 3.22: SEM images (magnification times: left column: $\times 50$; right column: $\times 500$.) of cast films from PLA solution with different ratio of DCM/THF (v/v) = 5). 1:4; 6). 0:5.

Film casting of different lignin derivatives

PLA/lignin derivative films were made by film casting of the mixed solution of 5 ml 30% PLA/DCM solution and 5 ml corresponding lignin derivative solution on Petri-dishes. They were then air-dried and studied by different analysis methods.

PLA, by itself, may not be the best solution for fertilizer coating because its hydrophilicity. It was also hard to form a good film on to the Petri dish in this study since the surface was full of pores. After mixing PLA with lignin and lignin derivatives, the situation has been changed. After esterification, all the films formed from modified lignin had relatively more homogeneous surface with no visible pores and cracks. It is therefore reasonable to say that the addition of different lignin had improved the PLA film quality by acting as a plasticizer to PLA, therefore increasing the film quality. Detailed film structures can be observed by SEM analysis. As seen in Figure 3.23a, unmodified lignin and PLA film shows uneven surface with grains. Since the original lignin had a bad dissolving property compared with the lignin derivatives, it had a higher potential to phase-separate from the PLA, which led to the uneven surface at the end. However, films were mostly flat under SEM observation after modification. AcSKL showed quite even surface. Even though the distribution of PaSKL (Figure 3.23e) in the film is uneven (maybe due to the incomplete mixing), the film still formed an even surface with only a small amount of nano-scale pores, while ManSKL (Figure 3.24a) formed a surface with big crystallized PLA chunks with gaps in between. In contrast, a perfect homogeneous layer was formed from LauSKL. Therefore, LauSKL (Figure 3.23g) has the best potential to be the reinforcement additives in PLA/lignin films. The structural and property differences among different derivatives are the main reason that caused the formation of different PLA films. Esterified lignin samples facilitated forming the films with relatively more even surface, while the Mannich reaction modified lignin seemed to weaken the effect.

Contact angle tests were also conducted on the different lignin/PLA films in order to see the impacts of modified lignin on surface wettability and film hydrophobicity of PLA. As seen in Table 3.7, the original PLA film has the lowest contact angle value of 52.30°, reflecting the natural hydrophilic property of PLA. With the addition of original SKL, the PLA/OriSKL (original SKL) film showed better water barrier property with a higher value of contact angle around 80.50°. It is reasonable to say that lignin has changed the hydrophobicity of the film because of

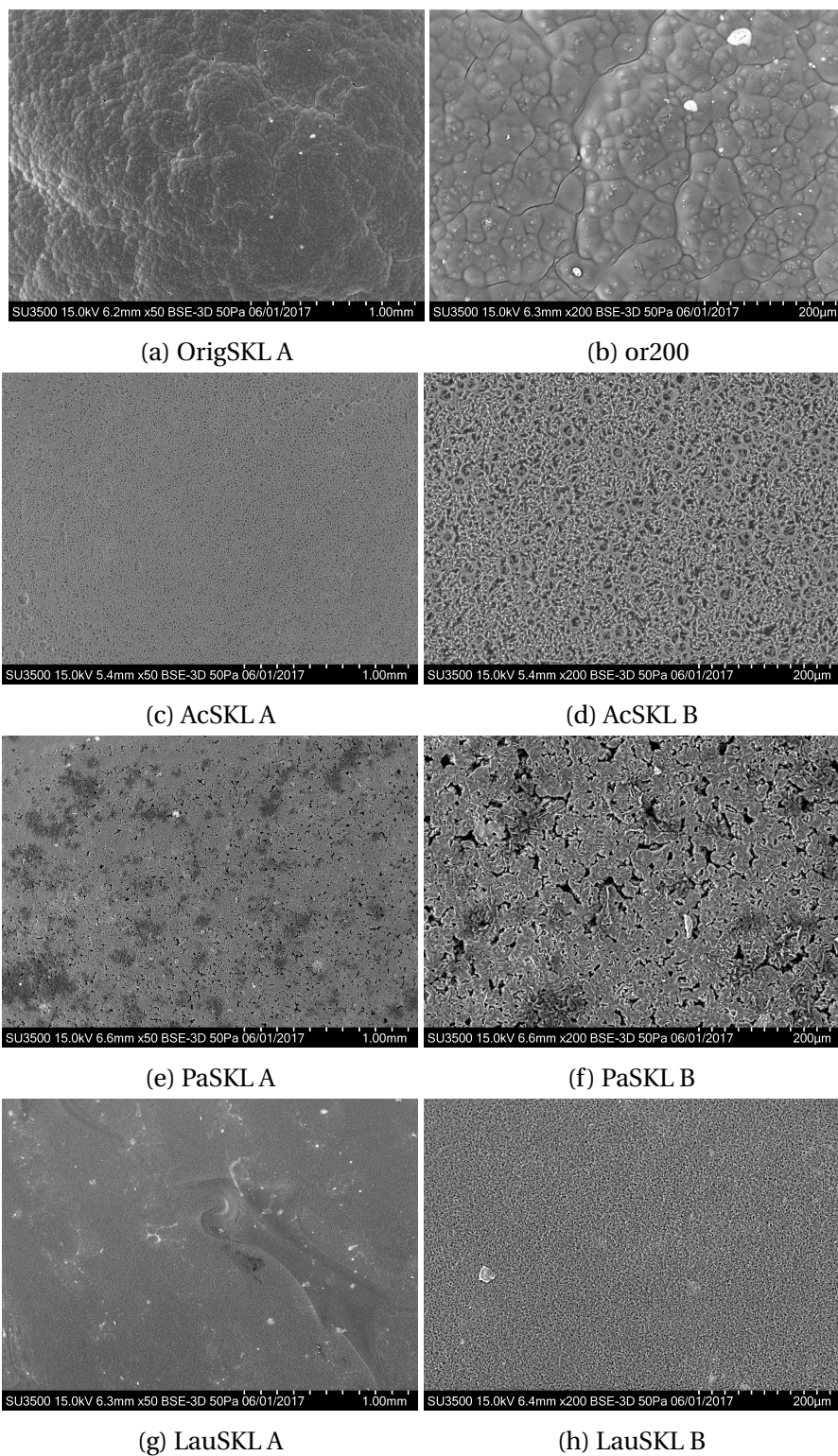


Figure 3.23: SEM images (magnification times: A: $\times 50$; B: $\times 200$) of cast films from PLA with original SKL and lignin derivatives.

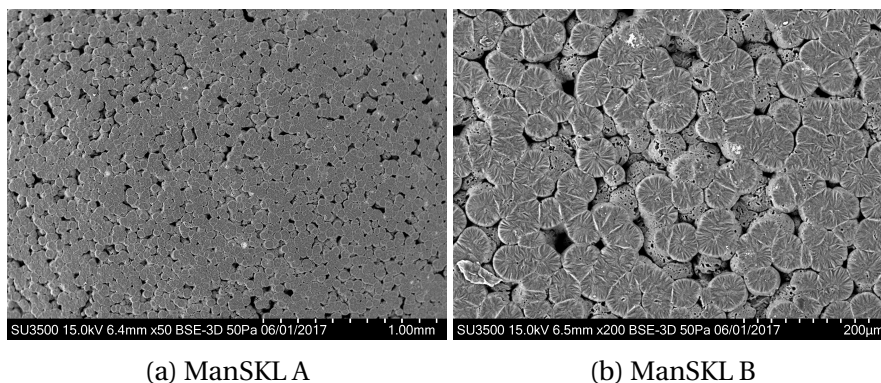


Figure 3.24: SEM images (magnification times: A: $\times 50$; B: $\times 200$) of cast films from PLA with original SKL and lignin derivatives.

its water barrier property (on account of multiple aromatic rings in the lignin structure). The final PLA/AcSKL, PLA/PaSKL and PLA/LauSKL films were less wettable (contact angle at 117.79° , 90.06° and 84.78° , respectively) than the original SKL/PLA film as expected. This may mainly due to the existence of grafted aliphatic chains in the modified lignin structures. On the other hand, the Mannich reaction gave the ManSKL/PLA film a lower contact angle value compared with the PLA/OriSKL, because the grafted diethylaminomethyl groups causing lignin sample with higher hydrophilic properties.

Table 3.7: Contact angle (θ) values of PLA (neat) film and PLA/derivative lignin complex films. (Unit: $^\circ$) (SD: Standard deviation).

Film type	PLA	PLA/OriSKL	PLA/AcSKL	PLA/PaSKL	PLA/LauSKL	PLA/ManSKL
Mean value	52.30	80.50	117.79	90.06	84.78	78.05
SD	2.02	1.81	2.36	1.04	5.09	1.52

3.2.3 Dip-coating results

LauSKL had the best film performance in SEM images, but AcSKL had better water barrier properties compared with LauSKL. Therefore, the observed properties of PLA/AcSKL complex were the best among the esterified samples. It was then selected together with the PLA/ManSKL complex to continue the following dip-coating study.

Figure 3.25a shows the typical SEM image of lignin/PLA coated urea pellet after dip-coating process. The coating layer is similar to the cast film, without pores and cracks on the surface.

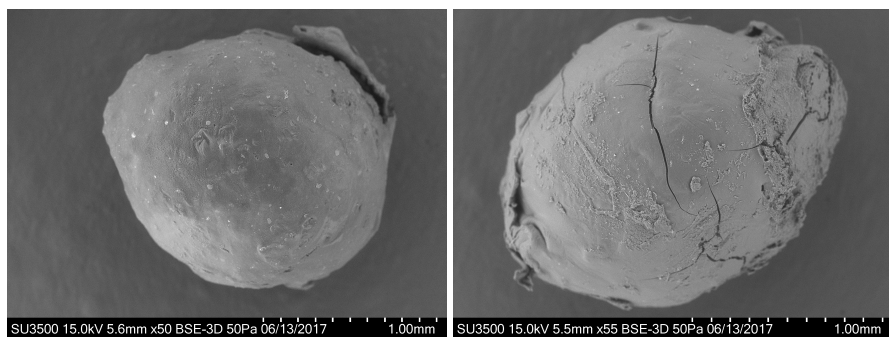
It is evenly distributed over the urea pellet. Then the dip-coating process was repeated two or three times in this study. The coating layer kept well distributed and compact with no clear imperfections. 50 pellets of urea were coated for each type of PLA/SKL and weighed and the mean values of weight increases were calculated accordingly (Figure 3.26). The quantity of coating layer was found well correlated to the repeating times. The average weight increases of urea pellets showed positive correlation with the repeating times, regardless the types of lignin derivatives used in the process. The coating layer showed single layer structure without separation and good attachment with the urea pellet regardless the repeating times. The thickness (around 9 μm) of the coating layer after three times coating can be found in Figure 3.25c, which was still quite thin compared to the size of urea core.

The coat layer was found to have a complete structure with only small cracks on the surface. It kept the shape of the urea (Figure 3.25b).

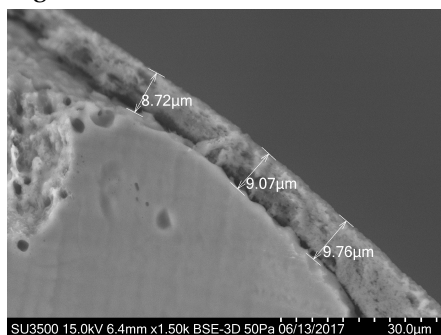
For the ManSKL coated urea pellet, the added lignin quantity can be calculated according to the average weight increase. Approximately 14-32 wt% of urea pellets were the coating layer of PLA/ManSKL after three times coating. The percentage of ManSKL was around 9.1 wt% in the PLA/ManSKL complex. ManSKL contains around 2.5 wt% N. The final coated urea pellets would have 0.0315-0.072 wt% organic bounded N.

3.2.4 Urea release

The coated urea pellets were then immersed in water and took out after the urea has been completely released in this study. Many articles (for example, Xian et al. (2009)) has used water immersion tests to evaluate the urea release condition and the method is to measure the release quantity of urea in the still water at different time intervals, and it is used as several national and international standards. This process usually requires more than 100 days of observation with more than 100g of urea pellets. The duration time and the small amount of coated urea prepared in this study limited the feasibility of this test. However, there was one interesting phenomenon during the water immersion tests which is able to be used as a general judgment criteria for the coating layer evaluation. The coated urea sinks in water since the thin coating layer is in a lower density than water, it was able to float on top of the water instead of sinking in after the urea core has been dissolved in the surrounded water. This gives a possibility to compare the effect



(a) Coated urea pellet before releasing (One time coating). (b) The pellet left after urea has been released in water.



(c) Coating layer over urea after three times coating.

Figure 3.25: SEM images of coating urea pellets.

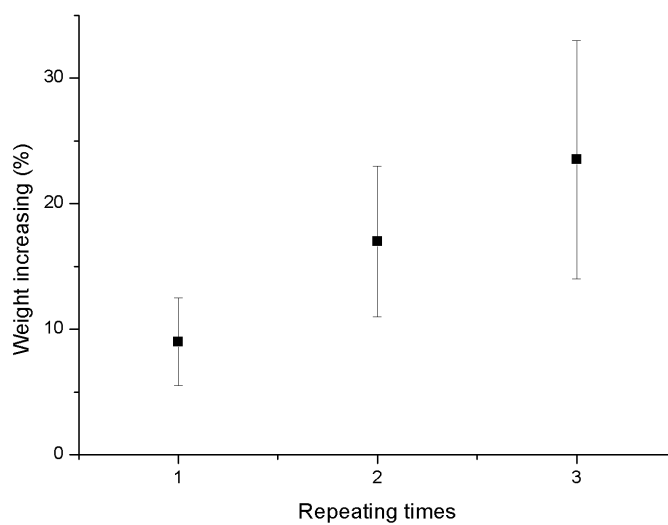


Figure 3.26: Average weight increases (in percentage) of urea pellets after coating by diverse PLA/lignin derivatives for 1, 2, and 3 times.

of different coating layers by recording the time when the floating was observed. In this study urea pellets were put individually into equal amount of water (25ml) and the starting time for floating has been recorded and compared.

Table 3.8: Results of floating time by different coating layers after the urea pellets have been put in water. (Unit: s) (SD: Standard deviation).

Coating layer type	PLA	PLA/AcSKL	PLA/ManSKL
Time (Mean value)(s)	253	2370	1650
SD (s)	63	195	142

Following data were obtained as listed in Table 3.8. The original urea pellets took approximately 50 s to be completely released in water (seen by the disappearance of the urea pellets). While for the sample after coating, the PLA coated pellets took approximately 250 s to be completely dissolved and floated, around 5 times longer than the one without coating. For the PLA/AcSKL ones, the coating layers floated after around 2370 s after they have been put in water, around 47 times as long as the bare urea. Similarly, PLA/ManSKL took around 1650 s to be released, a bit quicker than the PLA/AcSKL sample but still 33 times as long as the bare urea. In the real cases, the releasing process of urea pellets without coating may take several days (Hanafi et al. (2002)) when they were used in the soil. It may thus be expected that the releasing time will be prolonged when the lignin coated fertilizer are used in the soil.

On the other hand, even though 50 pellets have been used in this study to increase the reliability of the test results, it is still hard to give a firm evaluation of urea pellets to compare with the analysis by the international slow-released fertilizer standard. Under more practical conditions, fertilizers are almost totally covered by soil with no much surrounding water and the releasing will therefore also be influenced by the soil type. Better evaluations such as pot experiments (Li et al. (2014)) should be conducted in real soil.

Although the effects of lignin fictionalizations have not been verified by the real soil test in this study, there are some soil and fertilizer utilization influences that could be expected by the coated urea, according to Peng et al. (2004). Lignin was declared to give urea fertilizers higher efficiency by showing effects in nitrification inhibition which reduces N_2O emissions (83-96%). And the increased hydrophobicity of lignin will further lower the releasing speed of urea. The increasing of N amount in the lignin coating layer by ManSKL can be an effective slow-released

fertilizer by itself. Furthermore, it can also facilitate PLA by lowering the possibility of hydrolysis, which is the main defect of PLA during applications.

Chapter 4

Summary and Recommendations for Further Work

4.1 Summary and Conclusions

Industrial softwood kraft lignin (SKL) is a large scale available biopolymer and is valuable for coating urea together with polylactic acid (PLA). Modification of SKL before the coating application can improve the coating effects:

- Esterification of SKL lowers down the wettability of the coat layer, especially when using the modified SKL after acetylation, i.e. the AcSKL prepared.
- Mannich reaction-modification of SKL by diethylamine introduces organically bound nitrogen structure, termed ManSKL, which also becomes a slow-release type of N-fertilizer structure.
- Mannich reaction-modification of SKL by ethyleneaminetriacetic acid (ED3A) introduces further a metal chelating function for possible addition of essential trace element into the final fertilizer, although this has not been completely successful yet. Dip-coating technique is a simple alternative to the commonly utilized coating equipment. The method can be set up after:
 - Selection of solvent for the coating components. Dichloromethane (DCM) is the best for PLA and tetrahydrofuran (THF) is good for the modified SKL.
 - Optimization of concentration of coating components in the solvent. 30 % PLA in DCM is the best and 6 % modified SKL in THF is excellent.

- Optimization of mixed solvents for the PLA-modified SKL blend. DCM/THF ratio of 3/2 is the best.

After coating urea by PLA/modified SKL blend by dip-coating technique, the speed of urea releasing for the coated urea prepared is much slower than the un-coated or PLA-coated urea. The PLA/AcSKL and PLA/ManSKL coated urea are the best among all samples prepared, both with excellent properties in delaying the release of urea cores in water. The coated urea fertilizers prepared in this study have highly efficiency with excellent properties of water barrier, organically N slow release, and nitrification inhibition effect (due to the presence of free phenolic functional groups).

4.2 Recommendations for Further Work

There are several issues that can be improved to further enhance the preparation and/or efficiency of the slow-released fertilizers investigated in this study.

- In a short-term: Modification of the Mannich reaction conditions for preparation of ED3ASKL.

Here in this study, the reaction between ED3A and the lignin model compound, vanillyl alcohol gave sound results in coupling of ED3A onto the C₅ position. However, even though the G-units in SKL has the same structure as the model compound, there is still no clear coupling observed for the same reaction happening on SKL. In this study, only one experiment condition was used, and obviously more work on using varied conditions should be done in the near future.

- In a medium-term: Improvement of nitrogen release tests.

Due to the limitation of the available equipment facility and several other issues, more practical evaluation of urea release from the coated products has not been conducted in this study. Even though the coated layers showed better properties in hydrophobicity and better delay effects than the neat PLA layer, the results of the water immerse tests conducted in this study could be different in a large extent to the real release if the coated products are used in soil, since it has been known that the release speed can also be

strongly effected by the soil type and many other factors after the urea dissolution. Therefore, more complete urea release tests such as soil leaching and pot experiments (Li et al. (2014)) in artificial soil should be done in the future work.

- In a long-term: Machine design for dip-coating technique.

In this study, the dip-coating technique was conducted by hand and in a lab scale. However, if the dip-coating technique is going to be applied in a more controllable/repeatable manner and/or a larger scale, dip-coating machine design is going to be necessary. It can be expected that the design should be conducted in the lab scale first. Many factors have to be fully considered and optimized together with the design of the machine, such as viscosity of the PLA/lignin solution, evaporating speed of the coated layer, and ventilation system for the evaporated toxic solvents: DCM and THF and so on.

Bibliography

- Association of American Plant Food Control Officials, A. (1997). *Official Publication No.50, T-29*. Association of American Plant Food Control Officials, Inc.: West Lafayette, Indiana, USA.
- Bronson, K., Mosier, A., and Bishnoi, S. (1992). Nitrous oxide emissions in irrigated corn as affected by nitrification inhibitors. *Soil Science Society of America Journal*, 56(1):161–165.
- Brücher, J. (2010). Method for preparing slow release fertilizers. US Patent App. 13/382,240.
- Byrnes, B. (1990). Environmental effects of n fertilizer use—an overview. *Fertilizer Research*, 26(1-3):209–215.
- Chakar, F. S. and Ragauskas, A. J. (2004). Review of current and future softwood kraft lignin process chemistry. *Industrial Crops and Products*, 20(2):131–141.
- Chien, S., Prochnow, L., and Cantarella, H. (2009). Recent developments of fertilizer production and use to improve nutrient efficiency and minimize environmental impacts. *Advances in Agronomy*, 102:267–322.
- de Candolle, A. P. and de Candolle, A. (1844). *Théorie élémentaire de la botanique: ou, Exposition des principes de la classification naturelle et de l'art de décrire et d'étudier les végétaux*. Roret.
- Devassine, M., Henry, E., Guerin, P., and Briand, X. (2002). Coating of fertilizers by degradable polymers. *International Journal of pharmaceuticals*, 242(1):399–404.
- Du, X., Li, J., and Lindström, M. E. (2014). Modification of industrial softwood kraft lignin using mannich reaction with and without phenolation pretreatment. *Industrial Crops and Products*, 52:729–735.

- Finck, A. (1992). Fertilizers and their efficient use. *IFA (1992): World Fertilizer Use Manual*.
Editors: Halliday, DJ.
- Gellerstedt, G. (1992). Gel permeation chromatography. In *Methods in lignin chemistry*, pages 487–497. Springer.
- Goertz, H. (1993). Controlled release technology. *Kirk-Othmer encyclopedia of chemical technology*, 7(4):251–274.
- Granata, A. and Argyropoulos, D. S. (1995). 2-chloro-4, 4, 5, 5-tetramethyl-1, 3, 2-dioxaphospholane, a reagent for the accurate determination of the uncondensed and condensed phenolic moieties in lignins. *Journal of agricultural and food chemistry*, 43(6):1538–1544.
- Hahn, E. and Maxwell, D. (1952). Spin echo measurements of nuclear spin coupling in molecules. *Physical Review*, 88(5):1070.
- Hanafı, M., Eltaib, S., Ahmad, M., and Syed Omar, S. (2002). Evaluation of controlled-release compound fertilizers in soil. *Communications in soil science and plant analysis*, 33(7-8):1139–1156.
- Harris, R. K., Becker, E. D., Cabral de Menezes, S. M., Goodfellow, R., and Granger, P. (2001). Nmr nomenclature. nuclear spin properties and conventions for chemical shifts (iupac recommendations 2001). *Pure and Applied Chemistry*, 73(11):1795–1818.
- Hede, P. D., Bach, P., and Jensen, A. D. (2009). Fluidized-bed coating with sodium sulfate and pva-tio₂, 1. review and agglomeration regime maps. *Industrial & Engineering Chemistry Research*, 48(4):1893–1904.
- Johnson, C. (1999). Diffusion ordered nuclear magnetic resonance spectroscopy: principles and applications. *Progress in Nuclear Magnetic Resonance Spectroscopy*, 34(3):203–256.
- Jom pang, L., Thumsorn, S., On, J. W., Surin, P., Apawet, C., Chaichalermwong, T., Kaabbuathong, N., Narongchai, O., Srisawat, N., et al. (2013). Poly (lactic acid) and poly (butylene succinate) blend fibers prepared by melt spinning technique. *Energy Procedia*, 34:493–499.

- Karhunen, P., Mikkola, J., Pajunen, A., and Brunow, G. (1999). The behaviour of dibenzodioxocin structures in lignin during alkaline pulping processes. *Nordic Pulp & Paper Research Journal*, 14(2):123–128.
- Karhunen, P., Rummakko, P., Sipilä, J., Brunow, G., and Kilpeläinen, I. (1995). The formation of dibenzodioxocin structures by oxidative coupling. a model reaction for lignin biosynthesis. *Tetrahedron Letters*, 36(25):4501–4504.
- Lebo, S., Gargulak, J. D., and McNally, T. J. (2001). Lignin, kirk-othmer encyclopedia of chemical technology. *John Wiley & Sons, Inc. doi*, 10(1002):0471238961.
- Li, J., Hu, Y. S., Pu, L. M., Guo, G. S., and Niu, H. Y. (2014). Preparation of an environmental friendly slow release nitrogen fertilizer. In *Advanced Materials Research*, volume 1015, pages 346–349. Trans Tech Publ.
- Liitiä, T. M., Maunu, S. L., Hortling, B., Toikka, M., and Kilpeläinen, I. (2003). Analysis of technical lignins by two-and three-dimensional nmr spectroscopy. *Journal of agricultural and food chemistry*, 51(8):2136–2143.
- Lodhi, M. and Killingbeck, K. T. (1980). Allelopathic inhibition of nitrification and nitrifying bacteria in a ponderosa pine (*pinus ponderosa dougl.*) community. *American Journal of Botany*, pages 1423–1429.
- Mainka, H., Hilfert, L., Busse, S., Edelmann, F., Haak, E., and Herrmann, A. S. (2015). Characterization of the major reactions during conversion of lignin to carbon fiber. *Journal of Materials Research and Technology*, 4(4):377–391.
- Min, Z., Yuechao, Y., Fupeng, S., and Yanxi, S. (2005). Study and industrialized development of coated controlled release fertilizers [j]. *Journal of Chemical Fertilizer Industry*, 2:001.
- Mulder, W., Gosselink, R., Vingerhoeds, M., Harmsen, P., and Eastham, D. (2011). Lignin based controlled release coatings. *Industrial Crops and Products*, 34(1):915–920.
- Naz, M. Y. and Sulaiman, S. A. (2016). Slow release coating remedy for nitrogen loss from conventional urea: a review. *Journal of Controlled Release*, 225:109–120.

- Noellsch, A., Motavalli, P., Nelson, K., and Kitchen, N. (2009). Corn response to conventional and slow-release nitrogen fertilizers across a claypan landscape. *Agronomy Journal*, 101(3):607–614.
- Parker, B. A. and Cullen, B. A. (1994). N-acyl-n, n', n'-ethylenediaminetriacetic acid derivatives and process of preparing same. US Patent 5,284,972.
- Peng, J.-j., WANG, D.-h., and LIAO, Z.-w. (2004). Effect of lignin from paper-making black liquor on the transformation and the bio-utilization of urea-n [j]. *Journal of South China Agricultural University*, 1:006.
- Pereira, E. I., Da Cruz, C. C., Solomon, A., Le, A., Cavigelli, M. A., and Ribeiro, C. (2015). Novel slow-release nanocomposite nitrogen fertilizers: the impact of polymers on nanocomposite properties and function. *Industrial & Engineering Chemistry Research*, 54(14):3717–3725.
- Qiongxin Liu, Chaohui Zhou, H. Z. (2010). Method for preparing ethylene diamine triacetate. CN Patent 101,293,846.
- Sanchonx (2011). Ftir interferometer.
- Sarkanen, K. V. and Ludwig, C. H. (1971). *Liguins. Occurrence, formation, structure, and reactions*. New York.; Wiley-Interscience.
- Sato, S., Gondo, D., Wada, T., Kanehashi, S., and Nagai, K. (2013). Effects of various liquid organic solvents on solvent-induced crystallization of amorphous poly (lactic acid) film. *Journal of Applied Polymer Science*, 129(3):1607–1617.
- Shah, N., Sattar, A., Benanti, M., Hollander, S., and Cheuck, L. (2006). Magnetic resonance spectroscopy as an imaging tool for cancer: a review of the literature. *The Journal of the American Osteopathic Association*, 106(1):23–27.
- Shipway, P. (2006). The range of surface coating methods. *Surface Coatings for Protection Against Wear*. Ed. BG Mellor. Cambridge, England: Woodhead Publishing Ltd, pages 79–100.
- Sjostrom, E. (1981). Wood chemistry; fundamentals and applications. Technical report.

- Socrates, G. (2004). *Infrared and Raman characteristic group frequencies: tables and charts*. John Wiley & Sons.
- Södergård, A. and Stolt, M. (2010). Industrial production of high molecular weight poly (lactic acid). *Poly (Lactic Acid): Synthesis, Structures, Properties, Processing, and Applications*, pages 27–41.
- Tomani, P. (2010). The lignoboost process. *Cellulose Chemistry & Technology*, 44(1):53.
- TommyCP (2008). The mannich reaction.
- Trenkel, M. E. (1997). *Controlled-release and stabilized fertilizers in agriculture*, volume 11. International fertilizer industry association Paris.
- Wang, M., Sjöholm, E., and Li, J. (2017). Fast and reliable quantification of lignin reactivity via reaction with dimethylamine and formaldehyde (mannich reaction). *Holzforschung*, 71(1):27–34.
- Wenzel, R. N. (1936). Resistance of solid surfaces to wetting by water. *Industrial & Engineering Chemistry*, 28(8):988–994.
- Xian, C., Xiaoyun, M., Dehan, W., et al. (2009). Technology and effect of controlled-release fertilizer through physical-biochemical composite approaches. *Journal of Huazhong Agricultural University*.
- Yamamoto, C. F., Pereira, E. I., Mattoso, L. H., Matsunaka, T., and Ribeiro, C. (2016). Slow release fertilizers based on urea/urea–formaldehyde polymer nanocomposites. *Chemical Engineering Journal*, 287:390–397.
- Yi-zong, H., Zong-Wei, F., Fu—zhu, Z., and Shu—qin, L. Effects of lignin on nitrification in soil.
- Young, R. D. (1974). *TVA's development of sulfur-coated urea*. National Fertilizer Development Center, Tennessee Valley Authority.
- Yuan, T.-Q., Sun, S.-N., Xu, F., and Sun, R.-C. (2011). Characterization of lignin structures and lignin–carbohydrate complex (lcc) linkages by quantitative ¹³C and 2d hsqc nmr spectroscopy. *Journal of agricultural and food chemistry*, 59(19):10604–10614.

Appendix A

Calculation of OH from ^{31}P NMR spectra

^{31}P NMR spectroscopy is a quantitative way of measuring hydroxyl groups in the lignin samples. The measured ^{31}P NMR spectra was plotted with MestReNova program. Different peak areas after integral were analyzed using Microsoft Excel 2010. The peak areas of different OH to be calculated, A_{OH} , are usually obtained by setting area of internal standard (IS) equals to 1. By calculating the mole number of added IS, the final mole amount of hydroxyl groups can be gotten accordingly.

The first step is therefore to calculate the mole number of added IS. The internal standard (IS) of ^{31}P NMR in this study is N-hydroxy-5-norbornene-2,3-dicarboxylic acid imide pyridine. The concentration, c_{IS} , is 20 mg/ml. In this experiment, 0,1 ml IS (V_{IS}) has been added in each sample. With knowing the purity, P (%), and molar mass, M_{IS} (g/mol), of the IS, the amount (μmol) of IS (n_{IS}) added in each sample can be calculated as in equation A.1:

$$n_{IS} = \frac{c_{IS} \times V_{IS} \times P}{M_{IS}/1000} \quad (\text{A.1})$$

After obtaining results of n_{IS} , the second step is to calculate the amount of different hydroxyl groups (n_{OH}) in the lignin samples. Since all the samples were freeze dried before using, the dry content is 100 %. It is therefore reasonable to assume the dry weight of each sample kept the same as the weight of measurement. So n_{OH} (mmol/g) can be calculated according to equation A.2:

$$n_{OH} = \frac{A_{OH} \times n_{IS}}{1 \times W_{lignin}} \quad (\text{A.2})$$

Table A.1: Parameters of internal standard used in different samples.

Parameters	Weight of lignin	Dry content	Weight 100 % dry	c_{IS}	n_{IS}
unit(s)	mg	%	mg	mg/ml	μmol
Original	30.02	100.00	30.02	20.00	10.83
AcSKL	29.98	100.00	29.98	20.00	10.83
PaSKL	30.12	100.00	30.12	20.00	10.83
LauSKL	30.01	100.00	30.01	20.00	10.83
TFASKL	29.30	100.00	29.30	20.00	10.83
ManSKL	29.99	100.00	29.99	20.00	10.83

Table A.2: Calculated hydroxyl group values in different lignin samples.

Parameters	Aliphatic - OH		Condensed Ph - OH		H - OH		G - OH		Carboxyl - OH	
Unit(s)	Area	(mmol/g)	Area	(mmol/g)	Area	(mmol/g)	Area	(mmol/g)	Area	(mmol/g)
Original	5.29	1.91	5.55	2.00	0.67	0.24	6.20	2.24	1.20	0.43
AcSKL	0.08	0.03	0.00	0.00	0.00	0.00	0.00	0.00	0.96	0.35
PaSKL	0.24	0.09	0.13	0.05	0.00	0.00	0.00	0.00	8.45	3.04
LauSKL	3.28	1.18	3.72	1.34	0.00	0.00	3.93	1.42	6.83	2.46
TFASKL	2.19	0.81	2.26	0.84	0.00	0.00	2.73	1.01	0.04	0.01
ManSKL	4.72	1.70	3.62	1.31	0.00	0.00	0.00	0.00	0.59	0.21

Where W_{lignin} are the dry weights of different lignin samples.

Detailed information can be found in Table A.1 and Table A.2.

Appendix B

NMR spectra of ED3A

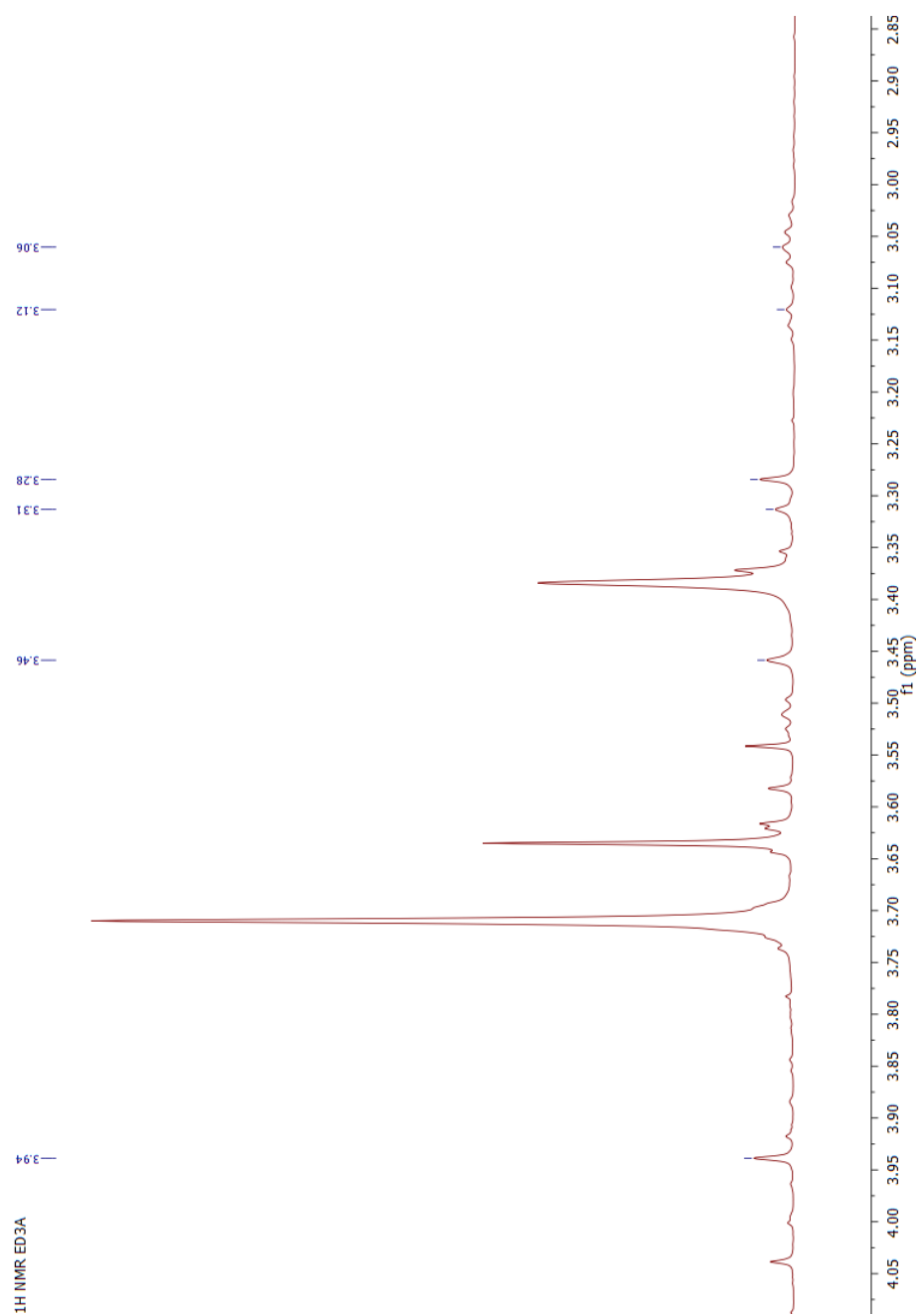


Figure B.1: ^1H NMR spectrum of synthesized ED3A solution.

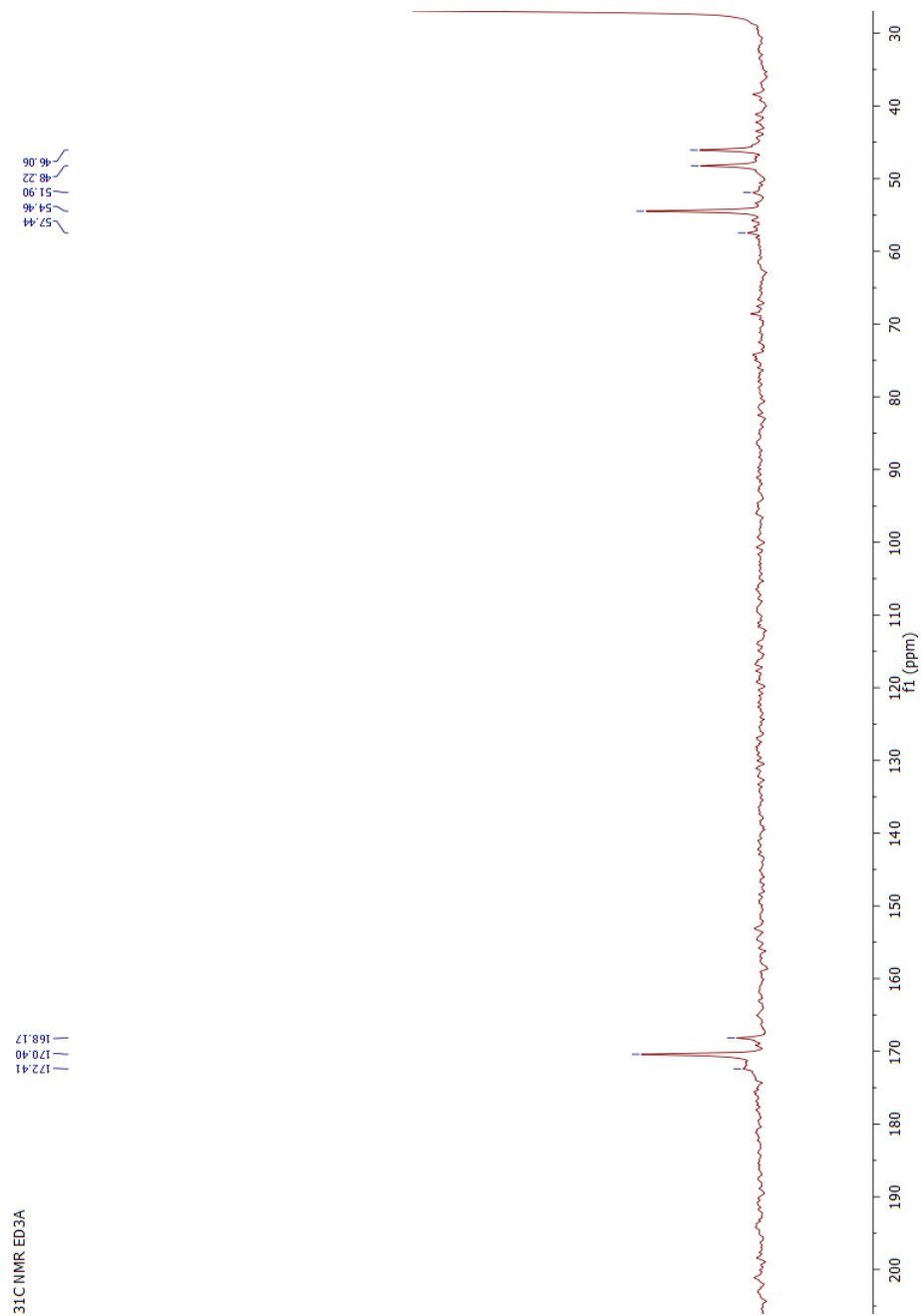


Figure B.2: ¹³C NMR spectrum of synthesized ED3A solution.